รายงานวิจัยฉบับสมบูรณ์

โครงการ: การวิเคราะห์ปริมาณธาตุในอนุภาคที่แขวนลอยในอากาศ แยกตามขนาดอนุภาค

Size Based Elemental Speciation of Airborne Particles by

Field-Flow Fractionation-Inductively Coupled Plasma Mass Spectrometry

โดย นางสาวอทิตยา ศิริภิญญานนท์ และคณะ

มิถุนายน 2548

สัญญาเลขที่ MRG4680005

รายงานวิจัยฉบับสมบูรณ์

โครงการ: การวิเคราะห์ปริมาณธาตุในอนุภาคที่แขวนลอยในอากาศ แยกตามขนาดอนุภาค

Size Based Elemental Speciation of Airborne Particles by

Field-Flow Fractionation-Inductively Coupled Plasma Mass Spectrometry

คณะผู้วิจัย	สังกัด
1. ดร. อทิตยา ศิริภิญญานนท์	ภาควิชาเคมี คณะวิทยาศาสตร์ มหาวิทยาลัยมหิดล
2. นางสาวอุษารัตน์ คำทับทิม	ภาควิชาเคมี คณะวิทยาศาสตร์ มหาวิทยาลัยมหิดล
3. นางสาวสุมัทนา วรปัญญานนท์	ภาควิชาเคมี คณะวิทยาศาสตร์ มหาวิทยาลัยมหิดล
4. รศ.ดร. ยุวดี เชี่ยววัฒนา	ภาควิชาเคมี คณะวิทยาศาสตร์ มหาวิทยาลัยมหิดล

สนับสนุนโดยทบวงมหาวิทยาลัย และสำนักงานกองทุนสนับสนุนการวิจัย

สารบัญ

Size Based Elemental Speciation of Airborne Particles by Field-Flow Fractionation-Inductively Coupled Plasma Mass Spectrometry

Abstract

Field-flow fractionation (FFF) is a gentle size separation technique applicable to both macromolecules and particles. Field-flow fractionation family comprises several sub-techniques, *i.e.*, flow-, sedimentation-, thermal-, and electrical-FFF. Two most commonly used FFF sub-techniques are flow-FFF (FlFFF) and sedimentation-FFF (SdFFF). Both FlFFF and SdFFF have been reported for environmental studies with the applicable size range of 2 nm-100 μm. The techniques provide wide range of information, including size and molecular weight distributions, diffusion coefficient, and polydispersity. In this study, SdFFF has been used to characterize size distribution of air particulate collected on the PM10 filter, and FlFFF has been employed to characterize size distribution of humic substances. In SdFFF experiment, various dispersing agents were tested and a 0.1% FL-70 with pH 8 was chosen as both dispersing agent and carrier liquid. The developed SdFFF method provided satisfactory separation efficiency and reproducibility (<3% RSD). Broad size distributions were obtained for air particulate samples collected from five locations. Nonetheless, peak maxima and distribution ranges of air particulates collected from one location were different from the others. Further, a hyphenated technique of SdFFF and inductively coupled plasma optical emission spectrometry (ICP-OES) was employed to study size-based elemental distribution of air particles. Aluminum, Fe, and Ti were detected across the whole size range of air particulate sample. With FlFFF, information on diffusion coefficient, size and molecular weight of humic substances was obtained. Moreover, aggregation of humic substances in Ca^{2+} and seawater was examined over suitable time interval. The aggregation was demonstrated by change of humic size distribution profile at a given pH value. With FlFFF-ICP-mass spectrometry (FlFFF-ICP-MS), associations of Cd, Cu, and Pb with humic aggregates were examined.

การวิเคราะห์ปริมาณธาตุในอนุภาคที่แขวนลอยในอากาศแยกตามขนาดอนุภาค

บทคัดย่อ

เทคนิค field-flow fractionation (FFF) เป็นเทคนิคที่สามารถใช้ในการแยกขนาดอนุภาคของมหโมเลกุลและอนุภาคต่าง ๆ โดยเทคนิคนี้ สามารถแบ่งย่อยเป็น flow-, sedimentation-, thermal-, และ electrical-FFF ซึ่งเทคนิค flow-FFF (FlFFF) และ sedimentation-FFF (SdFFF) สามารถนำมาประยุกต์ใช้กับการแยกขนาดอนุภาคได้มากมาย โดยเฉพาะอย่างยิ่ง อนุภาคสิ่งแวดล้อม โดยสามารถแยกอนุภาคในระดับ 2 นาโนเมตร ถึง 100 ไมโครเมตรได้ สามารถให้ข้อมูลต่าง ๆ เช่น ขนาดและการกระจายตัวของอนุภาค น้ำหนักโมเลกุลและการกระจายตัวของน้ำหนักโมเลกุล ค่าสัมประสิทธิ์การแพร่และดัชนีการกระจายตัวของขนาด ในงานวิจัยนี้ ได้ประยุกต์ใช้เทคนิค SdFFF สำหรับการวิเคราะห์ขนาดอนุภาคแขวนลอยในอากาศที่เก็บบนกระดาษกรองขนาด PM10 และใช้เทคนิค FlFFF สำหรับการวิเคราะห์การกระจายตัวของสารฮิวมิก ในการวิเคราะห์อนุภาคแขวนลอยในอากาศโดยใช้เทคนิคได้มีการทดลองเลือกสารกระจายตัวที่เหมาะสมสำหรับอนุภาคอากาศและพบว่า 0.1% FL-70 ที่ pH 8 มีความเหมาะสมในการนำไปใช้เป็นสารตัวพาและสารกระจายตัว โดยเทคนิค SdFFF ให้ค่าความแม่นยำในการวิเคราะห์ดี (มีค่า RSD น้อยกว่า 3%) ได้ทดลองวิเคราะห์อนุภาคแขวนลอยในอากาศจากแหล่งต่าง ๆ 5 แหล่ง พบว่าอนุภาคแขวนลอยในอากาศมีการกระจายตัวของขนาดอนุภาคกว้าง อย่างไรก็ดีอนุภาคอากาศจากแหล่งต่าง ๆ กันมีขนาดอนุภาคและการกระจายตัวของขนาดต่างกัน นอกเหนือจากนั้น ได้ใช้เทคนิค SdFFF-inductively coupled plasma optical emission spectrometry (SdFFF-ICP-OES) ในการวิเคราะห์การกระจายตัวของธาตุต่าง ๆ ตามขนาดต่าง ๆ ของอนุภาคแขวนลอยในอากาศ สำหรับการใช้เทคนิค FlFFF สามารถให้ข้อมูลเกี่ยวกับค่าสัมประสิทธิ์การแพร่ ขนาดอนุภาคและน้ำหนักโมเลกุลของสารฮิวมิก นอกเหนือจากนั้นได้ประยุกต์ใช้เทคนิค FlFFF ในการศึกษาเกี่ยวกับปรากฏการณ์การรวมตัวของสารฮิวมิกในสารละลาย Ca^{2+} และน้ำทะเล พบว่าสารฮิวมิกมีขนาดใหญ่ขึ้น และได้ใช้เทคนิค FlFFF-ICP-mass spectrometry (FlFFF-ICP-MS) ในการศึกษาการเกาะจับของ Cd, Cu และ Pb กับสารฮิวมิก

Executive Summary

1. **Project Title** Size Based Elemental Speciation of Airborne Particles by Field-Flow Fractionation-Inductively Coupled Plasma Mass Spectrometry

2. **Principal Investigator and Address**

Atitaya Siripinyanond

Department of Chemistry, Faculty of Science, Mahidol University

Rama VI Rd., Rajthevee, Bangkok 10400

Telephone 0-2201-5195, 0-2201-5129

Fax 0-2354-7151

E-mail: scasp@mucc.mahidol.ac.th

3. **Area** Analytical Chemistry

5. **Duration** 2 years

6. **Background Significance**

Challenges of analytical method developments in the field of trace element analysis recently have been focused on elemental speciation, which can either be based on particle size, redox properties, or chemical activities. From an environmental viewpoint, information about size-based elemental distribution is sought to gain insight into the mobility and transport of metal ions. The objective of this research project was therefore to develop analytical method, i.e., field-flow fractionation-inductively coupled plasma spectrometry, which could effectively provide information about size-based elemental speciation. Two types of samples were investigated, including air particulate matters, and humic substances.

The first part of this study concerns about size characterization of air particulate matters. Owing to the adverse effects of air particulates on the environment and human health, detailed knowledge about air particulate matters is needed. Air particulates can

cause serious problems by penetrating into human respiratory systems. Smaller particles are more harmful than the larger species, because they remain in the air for extended time, whereas the larger particles settle to the ground in a much faster manner. Therefore, small particles are more likely to get inhaled and transported into lungs. It is of prime importance to perform size-based elemental speciation of air particulate matters. The sedimentation field-flow fractionation-inductively coupled plasma optical emission spectrometry was proposed to provide useful information and was used in this study.

The second part of this study concerns about size characterization of humic substances. Understanding the humic substances is one of the central issues of environmental studies, since they play vital roles in the regulation of nutrient and toxic elements in terrestrial and aquatic environments. Only slight alterations in pH or ionic strength cause humic aggregation or flocculation. Detailed knowledge about humic aggregation phenomenon is still lacking. The use of flow field-flow fractionation-inductively coupled plasma mass spectrometry could provide information on humic aggregation and could be used to study metal interaction with humic substances.

7. Findings

Part I: Sedimentation field-flow fractionation-inductively coupled plasma optical emission spectrometry: size-based elemental speciation of air particulates

Details of particle size information and distribution ranges in sub-micrometer and micrometer regions can be obtained using SdFFF technique. With the use of ICP-OES as the element detector for the fractionated air particulates, the information about size-based elemental distribution of major elements in air particulates could be obtained. Four elements were investigated including Al, Fe, Mg, and Ti. Broad size distributions were observed for Al, Fe, and Ti with the mean diameters of approximately 1 μm, whereas narrower distribution profile was observed for Mg with the mean diameter of approximately 0.2 μm. Magnesium might be originally present in small size fractions of air particulate or it might be readily dissolved from the suspended air particulate. This observation suggested that Mg was more labile than other elements studied herein. Size distribution profiles of Al, Fe, and Ti were correlated well with the distribution profile of air particulate, suggesting that Al, Fe, and Ti were associated with all size fractions of air particulate sample. This could be

due to the fact that Al, Fe, and Ti are major elements in the earth crust, from where most dusts are derived.

Part II: Field-flow fractionation-inductively coupled plasma mass spectrometry: an alternative approach to investigate metal-humic substances interaction

Aggregation of a metal-spiked commercial Aldrich humic acid in an aqueous solution of calcium ion or in seawater was demonstrated by shifts in peak maximum of humic matter from smaller size (2.9 nm) to larger size (5.1 or 5.8 nm in Ca^{2+} solution or in seawater, respectively), and also by the broadening of size distribution profiles. With FFF-ICP-MS, associations of Cd, Cu, and Pb with humic aggregates were examined. The mean diameters of Cd-, Cu-, and Pb-bound humic aggregates in the metal-spiked humic acid were 4.1, 4.5, and 5.8 nm, respectively. These diameters were shifted to 6.0, 6.0, and 6.9 nm, respectively, in the humic acid incubated with calcium solution, whereas they were shifted to 6.5, 5.7, and 7.4 nm, respectively, in the humic acid incubated with seawater for 3 days. This study indicates that metal ions become less mobile in high salinity water, suggesting that metal mobility in fresh water should be faster than in estuarine or in seawater. The use of FIFFF-ICP-MS can be a comprehensive approach to help unravel the mystery of humic substances.

8. Output

8.1 Siripinyanond, A.; Worapanyanond, S.; Shiowatana, J. Field-flow fractionation-inductively coupled plasma mass spectrometry: an alternative approach to investigate metal-humic substances interaction, *Environ. Sci. Technol.* **2005**, *39*,3295-3301. (Journal Impact Factor 3.59)

8.2 Kumtabtim, U.; Shiowatana, S.; Siripinyanond, A. Sedimentation field-flow fractionation-inductively coupled plasma optical emission spectrometry: size based elemental speciation of air particulates, *J. Anal. Atom. Spectrom.*, submitted. (Journal Impact Factor 3.93)

หน้าสรุปโครงการ

1. **ชื่อโครงการ** การวิเคราะห์ปริมาณธาตุในอนุภาคที่แขวนลอยในอากาศ แยกตามขนาดอนุภาค

2. **ชื่อหัวหน้าโครงการ หน่วยงานที่สังกัด ที่อยู่ หมายเลขโทรศัพท์ โทรสาร และ** e-mail

นางสาวอทิตยา ศิริภิญญานนท์
อาจารย์ประจำภาควิชาเคมี คณะวิทยาศาสตร์ มหาวิทยาลัยมหิดล
ถนนพระรามที่ 6 เขตราชเทวี กรุงเทพ ฯ 10400
โทรศัพท์ 0-2201-5195, 0-2201-5129
โทรสาร 0-2354-7151
E-mail: scasp@mucc.mahidol.ac.th

3. **สาขาวิชาที่ทำการวิจัย** เคมีวิเคราะห์

5. **ระยะเวลาดำเนินงาน** 2 ปี

6. **ปัญหาที่ทำการวิจัย และความสำคัญของปัญหา**

การพัฒนาเทคนิคการวิเคราะห์ที่สามารถให้ข้อมูลนอกเหนือจากข้อมูลทางปริมาณ แต่ให้ข้อมูลเกี่ยวกับการกระจายตัวของปริมาณธาตุต่าง ๆ ในรูปฟอร์ม รูปลักษณะต่าง ๆ มีความสำคัญอย่างยิ่งยวด โดยที่การกระจายตัวของปริมาณธาตุตามรูปฟอร์มและรูปลักษณะนั้น รวมถึง ตามขนาดอนุภาค ตามคุณสมบัติรีดอกซ์ หรือตามคุณสมบัติทางเคมีต่าง ๆ ข้อมูลเกี่ยวกับการกระจายตัวของปริมาณธาตุตามขนาดอนุภาคต่าง ๆ เป็นข้อมูลที่มีความสำคัญในการใช้ทำนายและทำความเข้าใจเกี่ยวกับการเคลื่อนที่ของโลหะไอออนต่าง ๆ ในสิ่งแวดล้อม งานวิจัยนี้มีจุดประสงค์เพื่อพัฒนาเทคนิคการวิเคราะห์ field-flow fractionation-inductively coupled plasma spectrometry เพื่อใช้ในการให้ข้อมูลเกี่ยวกับการกระจายตัวของปริมาณธาตุตามขนาดอนุภาคต่าง ๆ ในตัวอย่างสำคัญ 2 ประเภท คือ อนุภาคแขวนลอยในอากาศ และ สารฮิวมิก

ส่วนแรกของงานวิจัย จะกล่าวถึงการกระจายตัวของปริมาณธาตุตามขนาดอนุภาคแขวนลอยในอากาศ งานวิจัยนี้มีความสำคัญเนื่องจากอนุภาคแขวนลอยในอากาศส่งผลกระทบโดยตรงต่อสิ่งแวดล้อมและสุขภาพของมนุษย์ หากมนุษย์หายใจอนุภาคแขวนลอยในอากาศเข้าไป อนุภาคขนาด

เล็กเป็นอันตรายมากกว่าอนุภาคขนาดใหญ่ เนื่องจากอนุภาคขนาดเล็กสามารถเดินทางไปสู่ปอดได้ ข้อมูลการกระจายตัวของปริมาณธาตุตามขนาดอนุภาคแขวนลอยในอากาศ จึงมีความสำคัญในการประเมินอันตรายจากอนุภาคแขวนลอยในอากาศ ซึ่งในงานวิจัยนี้ ได้ใช้เทคนิค sedimentation field-flow fractionation-inductively coupled plasma optical emission spectrometry ในการวิเคราะห์ให้ข้อมูลดังกล่าว

ส่วนที่สองของงานวิจัยกล่าวถึง การกระจายตัวของปริมาณธาตุตามขนาดอนุภาคต่าง ๆ ของสารฮิวมิก งานวิจัยนี้มีความสำคัญเนื่องจากสารฮิวมิกมีบทบาทที่สำคัญในการเคลื่อนย้ายธาตุต่าง ๆ ที่มีประโยชน์และเป็นพิษในสิ่งแวดล้อม เนื่องจากสารฮิวมิกอาจเกิดการรวมตัวเป็นอนุภาคที่ใหญ่ขึ้นได้ในเมื่อตัวกลางมีค่าความเป็นกรด-ด่าง หรือมีไอออนละลายอยู่แตกต่างกันไป ความสามารถในการเคลื่อนที่ในสิ่งแวดล้อมของสารฮิวมิกและการเคลื่อนย้ายธาตุต่าง ๆ ก็เปลี่ยนไปด้วย งานวิจัยนี้จึงมีจุดประสงค์เพื่อประยุกต์ใช้เทคนิค flow field-flow fractionation-inductively coupled plasma mass spectrometry ในการศึกษาคุณลักษณะต่าง ๆ ของสารฮิวมิก

7. ข้อมูลที่ค้นพบจากงานวิจัย

ส่วนที่ 1 *Sedimentation field-flow fractionation-inductively coupled plasma optical emission spectrometry: size-based elemental speciation of air particulates*

เทคนิค sedimentation field-flow fractionation สามารถให้ข้อมูลเกี่ยวกับขนาดอนุภาคและการกระจายตัวของขนาดอนุภาคต่าง ๆ ในระดับไมโครเมตรและระดับที่เล็กกว่าไมโครเมตร เมื่อใช้เทคนิค sedimentation field-flow fractionation ร่วมกับ inductively coupled plasma optical emission spectrometry สามารถให้ข้อมูลเกี่ยวกับการกระจายตัวของธาตุตามขนาดอนุภาคแขวนลอยในอากาศได้ โดยในงานวิจัยนี้ ได้ศึกษา ธาตุ 4 ชนิด คือ Al, Fe, Mg, และ Ti พบว่า Al, Fe, และ Ti มีการกระจายของขนาดอนุภาคที่กว้าง โดยมี-ขนาดอนุภาคเฉลี่ย 1 ไมโครเมตร ในขณะที่ Mg มีการกระจายของขนาดอนุภาคแคบและมีขนาดอนุภาคเฉลี่ย 0.2 ไมโครเมตร ทั้งนี้กล่าวได้ว่า Mg เกาะกับอนุภาคอากาศขนาดเล็ก ส่วนธาตุอื่น ๆ เกาะอยู่ทั่วทุกขนาดอนุภาค

ส่วนที่ 2 *Field-flow fractionation-inductively coupled plasma mass spectrometry: an alternative approach to investigate metal-humic substances interaction*

เทคนิค flow field-flow fractionation สามารถให้ข้อมูลเกี่ยวกับการรวมตัวของสารฮิวมิก โดยพบว่าสารฮิวมิกเกิดการรวมตัวในตัวกลางที่มี Ca^{2+} ละลายอยู่ หรือในตัวกลางน้ำทะเล สังเกตได้จากขนาดอนุภาคของสารฮิวมิกเปลี่ยนจาก 2.9 นาโนเมตร เป็น 5.1 และ 5.8 นาโนเมตร ในตัวกลางสารละลาย Ca^{2+} และน้ำทะเลตามลำดับ โดยเทคนิค flow field-flow fractionation-inductively coupled plasma mass spectrometry สามารถให้ข้อมูลเกี่ยวกับการเกาะจับของ Cd, Cu, และ Pb กับสารฮิวมิก โดยขนาดอนุภาคของ Cd-bound humic aggregates, Cu-bound humic aggregates, และ Pb-bound humic aggregates เป็น 4.1, 4.5, และ 5.8 นาโมเมตร ตามลำดับ และขนาดอนุภาคใหญ่ขึ้นเป็น 6.0, 6.0, และ 6.9 นาโนเมตร ตามลำดับในสารละลาย Ca^{2+} และ 6.5, 5.7, และ 7.4 นาโนเมตร ตามลำดับในน้ำทะเล งานวิจัยนี้ชี้ให้เห็นว่าไอออนของโลหะมีความสามารถในการเคลื่อนที่ในสิ่งแวดล้อมได้ช้าลงในตัวกลางที่มีความเค็มสูง พิจารณาจากขนาดที่ใหญ่ขึ้น อาจกล่าวสรุปได้ว่าไอออนของโลหะสามารถในการเคลื่อนที่ในน้ำจืดได้เร็วกว่าน้ำเค็ม

8. ผลงานวิจัยที่ตีพิมพ์ในวารสารวิชาการระดับนานาชาติ

ได้ส่งผลงานวิจัยที่เกี่ยวข้องกับโครงการเพื่อตีพิมพ์ในวารสารนานาชาติ จำนวน 2 เรื่อง โดยที่ได้ตีพิมพ์แล้ว 1 เรื่อง ส่วนอีก 1 เรื่อง กำลังรอผลการพิจารณา

8.1 Siripinyanond, A.; Worapanyanond, S.; Shiowatana, J. Field-flow fractionation-inductively coupled plasma mass spectrometry: an alternative approach to investigate metal-humic substances interaction, *Environ. Sci. Technol.* **2005**, *39*,3295-3301. (Journal Impact Factor 3.59)

8.2 Kumtabtim, U.; Shiowatana, S.; Siripinyanond, A. Sedimentation field-flow fractionation-inductively coupled plasma optical emission spectrometry: size based elemental speciation of air particulates, *J. Anal. Atom. Spectrom.*, submitted. (Journal Impact Factor 3.93)

บทที่ 1

Sedimentation field-flow fractionation-inductively coupled plasma optical emission spectrometry: size-based elemental speciation of air particulates

Abstract

The applicability of sedimentation field-flow fractionation-inductively coupled plasma optical emission spectrometry (SdFFF-ICP-OES) was investigated for elemental size characterization of PM_{10} air particulates. The effects of various dispersing agents and pH values on dispersion stability of air particulates were examined by zeta potential measurement. Anionic surfactants, which were 0.1% FL-70 and 0.1% SDS, exhibited the zeta potential values of more negative than -30 mV, suggesting that both surfactants could efficiently disperse air particulates. A 0.1% FL-70 with pH 8 was chosen as both dispersing agent and carrier liquid. The developed SdFFF method provided satisfactory separation efficiency and reproducibility (<3% RSD). Broad size distributions were obtained for air particulate samples collected from five locations. Nonetheless, peak maxima and distribution ranges of air particulates collected from one location were different from the others. Further, a hyphenated technique of SdFFF and ICP-OES was employed to study size-based elemental distribution of air particles. An ultrasonic nebulizer was used in order to increase sample transport efficiency and hence improve the sensitivity of ICP-OES detection. Aluminum, Fe, and Ti were detected across the whole size range of air particulate sample.

Introduction

Owing to the adverse effects of air particulates on the environment and human health, recent studies have been concerned with chemical compositions, emission sources, and size distributions of air particulates. Smaller particles are more harmful than the larger ones, because they remain in the atmosphere for extended time, whereas the larger particles settle to the ground in a much faster manner [1-3]. Therefore, small particles (less than 10 or 15 μm in size) are more likely to get inhaled and transported into lungs [4]. Various size characterization tools for air particulate exist, including cascade impactor, electric low pressure impactor, electrical aerosol analyzer (EAA), and scanning mobility particle sizer (SMPS) [5]. All these methods possess both advantages and disadvantages in terms of analysis time, reproducibility, sensitivity, cost, and etc [6]. Recently, an alternative

technique, sedimentation field-flow fractionation (SdFFF) also has been reported for size characterization of soot and urban airborne particles [7,8]. Sedimentation field-flow fractionation is a powerful technique for fractionation and characterization of particles and colloids in environmental and biological samples [5,9,10]. For environmental samples, colloidal particles in river water [11], colloidal aggregates [12], soil particles [13], and airborne samples [5-8,14,15] were investigated.

Airborne particles contain various elements such as Al, Ca, Cu, Fe Mg, Ni, Pb, and Zn. Studies of size distribution and elemental composition of air particulate have been reported by several investigators [16-18]. It has been indicated that the most toxic elements tend to be most abundant in the smallest particles [19,20]. Gaining the information about size-based metal distributions in aerosols or air particulate samples should thus be worthwhile for the understanding of its toxicity. The goal of this study was to develop an efficient analytical method to perform size separation of air particulates with on-line element detection using a combined technique of SdFFF and inductively coupled plasma optical emission spectrometry (ICP-OES).

Theory

Separation by sedimentation FFF (SdFFF) is achieved by applying centrifugal field force on the particles suspended in a carrier liquid [21]. The centrifugal force causes sedimentation of the sample components, according to the product of their effective volume and density difference between the suspended particles and carrier liquid. In the SdFFF channel, particles are distributed between different axial flow vectors according to the balance between the applied centrifugal field and diffusion of the particles. By knowing the exact geometry of the SdFFF channel, the field, flow rate, and the density difference between particle and carrier liquid, diameter of the separated particle (d) can be calculated using Equation 1 [22],

$$d = \left(\frac{36kT}{\pi G w \Delta \rho V_m} \right)^{1/3} V_r^{1/3} \qquad (1)$$

where k is the Boltzmann's constant, T is an absolute temperature, G is an angular acceleration ($G = \omega^2 r$, where ω is an angular velocity around radius r), w is a channel thickness, $\Delta\rho$ is the density difference between particle and carrier liquid, V_m is a channel void volume, and V_r is a retention volume of the separated particle. In practice, a set of standards of known particle sizes is generally used for SdFFF channel calibration. Relationship between the particle diameter (d) and elution time (t_r) can be expressed in Equation 2 [23],

$$\log t_r = S_d \log d + \log t_{r1} \quad (2)$$

where S_d is a size-based selectivity, and $\log t_{r1}$ is a constant equal to the extrapolated value of t_r for particles of a unit diameter. Once the calibration function as described in Equation 2 is obtained experimentally, a diameter of unknown particle can be calculated from the retention time provided that the densities of standard and sample particles are equal. In case that the densities of sample and standard are different, the density compensation theory must be applied by adjusting the field strength used in the separation as shown in Equation 3 [23],

$$(\sqrt{\Delta\rho}.\mathrm{rpm})_1 = (\sqrt{\Delta\rho}.\mathrm{rpm})_2 \quad (3)$$

where rpm represents the applied centrifugal field, and subscripts 1 and 2 represent the standard and the sample, respectively. Subsequently, a raw fractogram can be converted to particle size distribution by Equation 4 [23],

$$m(d) = c(t_r)\frac{dV_r}{dd} = c(t_r)\dot{V}\left|\frac{dt_r}{dd}\right| \quad (4)$$

where m(d) is the mass-based size distribution, $c(t_r)$ is the fractogram signal, and V is the flow rate.

Experimental

Instrumentation

The SdFFF system was a model S101 Colloid/Particle Fractionator (Postnova Analytik, Germany). The channel length, breadth, and thickness were 89.5 cm, 2.0 cm, and 0.0254 cm, respectively. The rotor radius was 15.1 cm with the total channel volume of 4.5 mL. The carrier solution was introduced into the SdFFF channel by an HPLC pump (PN1122, Postnova Analytik, Germany). The elution of particles was monitored by a UV/VIS detector (Model UV-2000 Spectra SYSTEM) at a fixed wavelength of 254 nm. Samples were introduced into the channel via an injection valve (Rheodyne) with a fixed loop of 100 μL. All SdFFF measurements were performed using a power programming mode to reduce the time necessary for analysis. The operating conditions for SdFFF run are summarized in Table 1. An end-on view ICP-OES system (Spectro Ciros, Germany) was used to detect elements in the fractionated air particulates as illustrated in Figure 1. An ultrasonic nebulizer with a desolvation system model U-5000 AT (CETAC Omaha, NB, USA) was used. Owing to the similarity of the SdFFF channel flow and ICP-OES sampling flow rates typically used for analysis, the ultrasonic nebulizer was connected directly to the UV detector outlet with a 50-cm length of poly(tetrafluoroethylene) tubing (PTFE, 0.58 mm id). The operating conditions of ICP-OES measurements are summarized in Table 1.

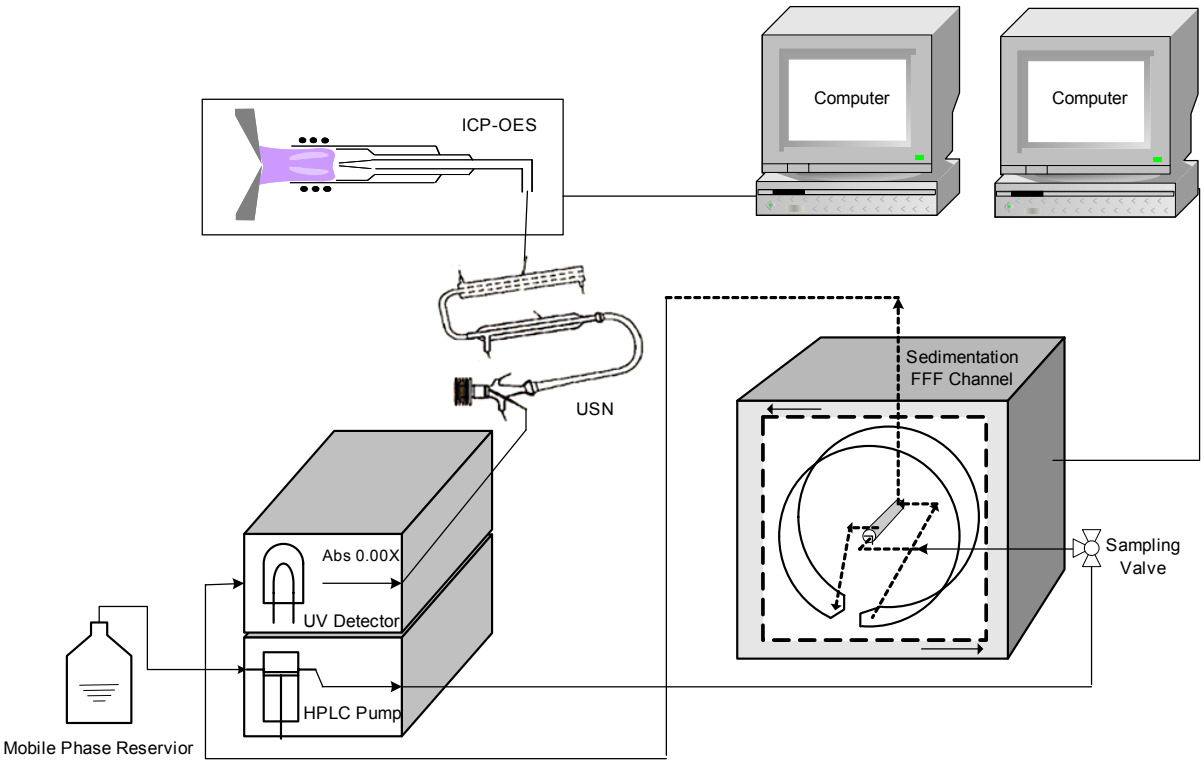

Figure 1 Schematic diagram illustrating SdFFF-ICP-OES set up.

To measure the zeta potential values of a sample dispersed in various dispersing agents, a model DTS 5300 zeta potential analyzer (Malvern Instruments, Worcestershire, United Kingdom) was used.

Table 1 SdFFF-ICP-OES operating conditions

SdFFF operating conditions	
SdFFF channel dimensions/cm^3	89.5 x 2.0 x 0.0254
SdFFF rotor radius/cm	15.1
Carrier liquid	0.02% (v/v) FL-70 containing 0.02% (w/v) sodium azide
Channel flow rate/ mL min^{-1}	1.5
Equilibration time/ min	15
Power field programming	initial field strength, 700 rpm for 5 min; field decay parameter, -40; final field strength, 20 rpm
ICP-OES operating conditions	
Rf generator frequency/ MHz	27.2
Rf power/ W	1350
Nebulizer gas flow rate/ L min^{-1}	0.8
Coolant gas flow rate/ L min^{-1}	12.0
Auxiliary gas flow rate/ L min^{-1}	1.0
Lines monitored/ nm	Al (167.07), Fe (239.50), Mg (279.55), and Ti (334.94)
Ultrasonic nebulizer conditions	
Heater temperature/ ^{o}C	140
Condenser temperature/ ^{o}C	5
Desolvator heating temperature/ ^{o}C	160
Sweep gas flow rate/ L min^{-1}	2.0

Materials and reagents

All polystyrene latex standards (0.53, 0.72, and 1.00 μm) used in this work were purchased from Postnova Analytik for SdFFF system calibration. The standards were diluted with 0.1% FL-70 to obtain the final solid contents of 0.01%(w/v) before injection into the SdFFF channel. Various dispersing agents, both non-ionic and anionic types, were tested. The non-ionic surfactant included Triton X-100 (Fluka Chemicals, Switzerland) and Tween 20 (Fluka Chemicals), whereas the anionic surfactant included FL-70 (Fisher Scientific, Pittsburgh, PA, USA) and sodium dodecyl sulfate (SDS, Fluka Chemicals). All dispersing agents were prepared to have the final concentration of 0.1% before use.

The PM_{10} air particulate samples were collected using a high volume air collector and all the samples were kindly provided by the Pollution Control Department (Bangkok, Thailand). The density of air particulates was assumed to be the same as that of polystyrene latex bead, i.e., 1.05 g cm^{-1}.

Sample preparation for SdFFF analysis

A quartz fiber filter containing air particulates was cut into small pieces (0.5 cm x 0.5 cm) and placed in a 100 mL beaker with approximately 30 mL of 0.1% FL-70. It was then sonicated in an ultrasonic bath (Branson Ultrasonics Corporation, CT, USA) for 10 minutes to remove the air particles from the filter. All fiber filter pieces were removed from the beaker by a Teflon forceps and the suspended air particulates were transferred into a centrifuge tube and centrifuged at 3,500 rpm for 30 min. The supernatant part was taken out from the centrifuge tube and the bottom part containing air particulates were made up volume to 1.5 mL by adding the appropriate dispersing agent, which was 0.1% FL-70. The suspended air particulates (0.3%, w/v) were sonicated for 20 min and vortexed for 1 min before introduction into the SdFFF channel. It should be noted that only approximately 80% could be extracted out from the filter. Therefore, the suspended air particulates used in this study might not be the true representation of the original samples. Nonetheless, the main objective of this study was to develop the method used for size separation with

simultaneous element detection. Therefore, the truly representative sample was not required.

To illustrate the separation capability of the SdFFF method, the fractionated air particulates were collected at three different retention times (repeatedly 8 times). The fractionated air particulates were transferred into a centrifuge tube and centrifuged at 3,500 rpm for 30 min. The supernatant was decanted off and a 0.1% (v/v) FL-70 was added to air particulates to obtain the final volume of 0.25 mL. The fractionated air particulates were sonicated for 20 min and mixed by vortex for 1 min before re-injection into the SdFFF channel to reexamine the size distribution.

Sample preparation for zeta potential measurement

To examine dispersing ability of various surfactants for air particulate samples, the zeta potential values were measured. For the zeta potential measurement, various dispersing agents containing 0.1% of surfactant and 0.02% (w/v) of sodium azide added as bacteriocide were tested. The pH values of dispersing agents were adjusted to 6 and 8. Air particulate samples were prepared as described earlier, but the concentrations of samples were 0.2% (w/v).

Results and discussion

SdFFF channel calibration

The SdFFF channel was tested and calibrated with polystyrene latex standards of known particle sizes. By calibrating the SdFFF channel with these particle size standards, a calibration equation was obtained as follows: $\log t_r = 0.877 \log d + 1.44$, $R^2 = 0.9898$. This equation was used to translate the retention time to the diameter scale. The slope is termed “size selectivity”, which is a measure of the SdFFF ability to separate two components [23].

Choices of dispersing agent and carrier liquid

A proper dispersing agent must be carefully selected to minimize flocculation of air particulates caused by particle-particle interaction [24]. Also, a suitable carrier liquid for SdFFF separation of air particulate samples must be used to reduce particle-particle and particle-wall interactions. In this study, the effect of various surfactants on dispersion stability of air particulates was evaluated by considering the zeta potential values.

The zeta potential values of more than +30 mV or less than -30 mV indicate the stable dispersion of particles. High zeta potential values indicate high degree of electrostatic repulsion, whereas low zeta potential values indicate high degree of van der Waals attraction, which subsequently causes sample flocculation. Table 2 shows that a 0.1% FL-70 at pH 8 and 0.1% SDS at pH 6 and 8 could efficiently disperse the air particulates. This suggests that anionic surfactant is more efficient than non-ionic surfactant for dispersion of airborne particles. In this work, the 0.1% SDS was not used because it contained high concentrations of analyte elements and elevated the background intensities of analyte elements when measured with ICP-OES. With the selected dispersing agent and carrier liquid, which was a 0.1% FL-70, reproducibility of the fractionation was evaluated by examining the selected air particulate sample. The retention time was found to be 16.9 $\pm$ 0.3 min (n = 4), with the corresponding diameter value of 0.34 $\pm$ 0.01 μm, yielding the %RSD of less than 3.

Table 2 Zeta potential values of air particulate dispersed in various dispersing agents. The sample was collected from a heavy traffic area in Bangkok.

Dispersing agents	Type of surfactant	Zeta potential (mV)	
		at pH 6	at pH 8
0.1%TritonX-100	non-ionic	-15.5	-22.8
0.1%Tween 20	non-ionic	-9.9	-12.6
0.1%FL-70	anionic	-21.1	-33.7
0.1%SDS	anionic	-33.4	-37.2

Separation performance of SdFFF

A power programming SdFFF was used for size separation of air particulate samples with three experimental conditions, using various initial field strengths (500, 700, and 900 rpm), with other operating conditions fixed. The resulting fractograms of air particulates and the correlated size and cumulative area distributions are shown in Figure 2. The peak maxima and size distribution patterns of air particulates obtained from three different operating conditions were similar (Figure 2b), implying that reliable size information were obtained using SdFFF. In addition, the diameters at 50% cumulative area (~1.03 μm) obtained from different initial field strengths were in excellent agreement, indicating good performance of the SdFFF method (Figure 2c). Since the particle size information obtained from three different initial field strengths were similar, the initial field strength of 700 rpm was used for subsequent analysis to ensure baseline separation with reasonable analysis time (~60 min).

Since monomodal fractograms and size distribution patterns were obtained (Figures 2a and 2b), one might wonder if SdFFF really separated the particle. To illustrate the separation ability of SdFFF, the fractionated air particulate samples (Figure 3) were collected at three different retention times (repeatedly 8 injections) and the fractionated air particulates were re-injected into the SdFFF channel as described in the experimental section. Fractograms of the fractionated air particulates collected at different retention times are shown in Figure 3b. The fractograms of each fractionated air particulate exhibited peak maximum at different retention times, corresponding to the retention times when the fractions were collected. Therefore, this study confirms that good separation of air particulate was achieved by SdFFF method.

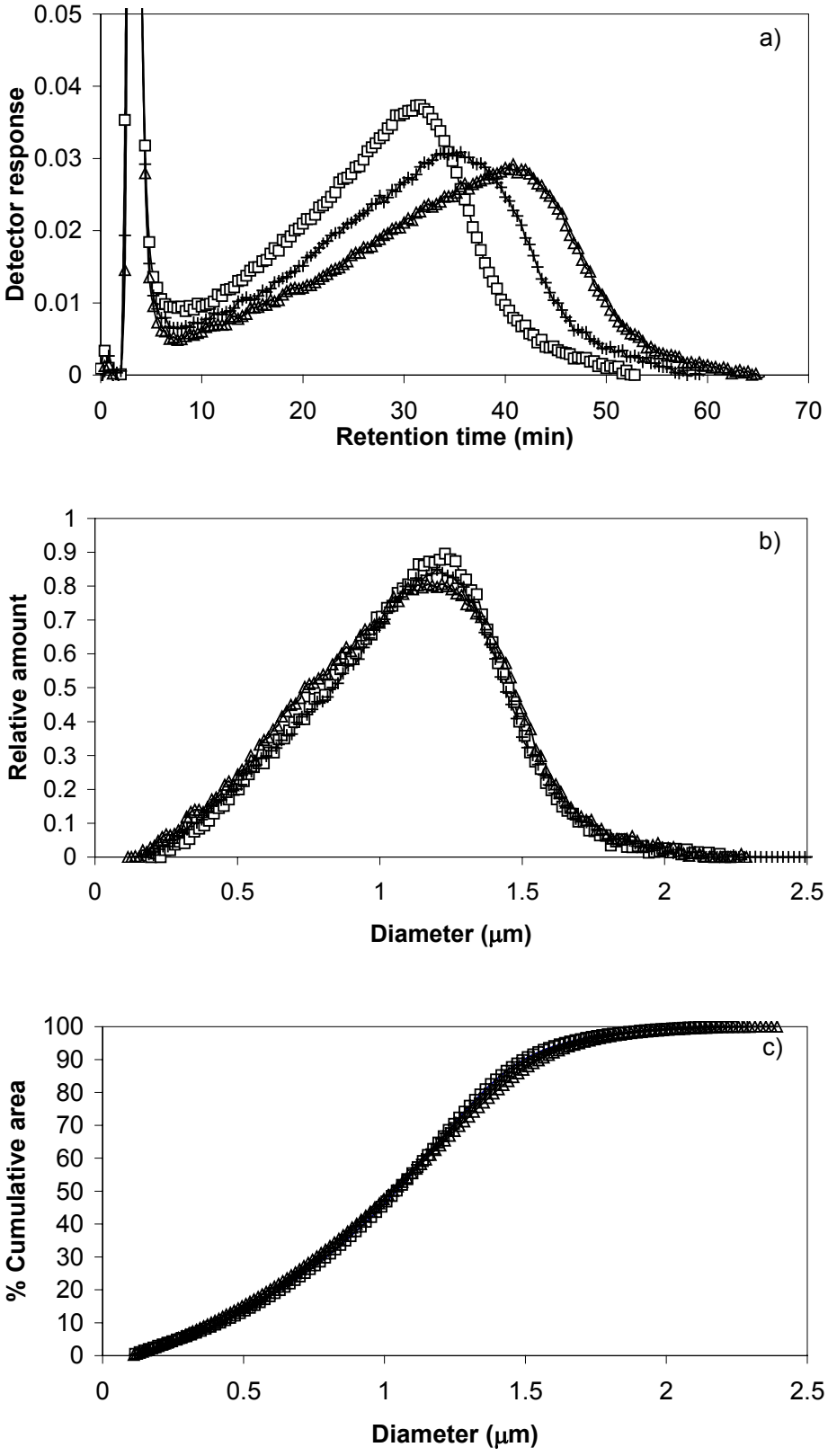

Figure 2 a) Fractograms of air particulate obtained from SdFFF run at initial field strengths of 500 rpm (□), 700 rpm (+), and 900 rpm (△); b) the size distributions; and c) the cumulative plots obtained from the corresponding initial field strengths.

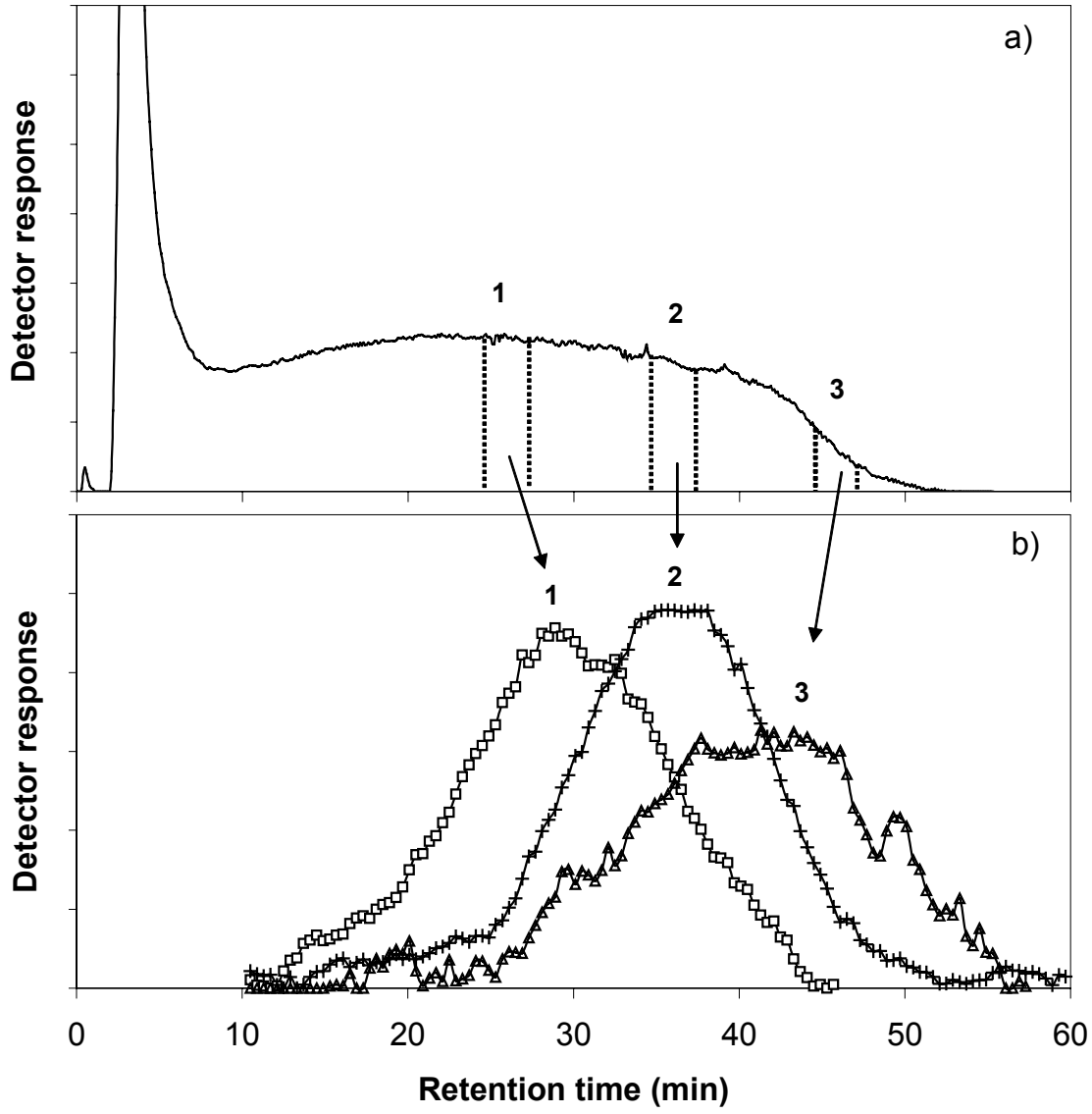

Figure 3 Fractograms of air particulate: (a) the original fractogram; and (b) fractograms of the fractionated air particulates, by which 1 (□), 2 (+), and 3 (△) are the fractions of air particulate collected from the original separation at the retention times of 25-28, 35-38, and 45-48 min, respectively.

Size distributions of air particulates from various locations

Particle size distributions and the corresponding cumulative area plots of air particulate samples collected from five different locations are illustrated in Figure 4. Broad size distributions of air particulates were obtained for all samples. Nonetheless, air particulates collected from different locations exhibited different peak maxima and distribution ranges. Considering the cumulative plots of air particulates, samples collected from locations 1 and 2 exhibited mean diameters at approximately 0.6 μm, whereas samples collected from locations 3-5 exhibited mean diameters at approximately 1.1 μm (the mean diameter value was determined from the cumulative plot by measuring the diameter at 50% cumulative area, as illustrated in Figure 4b). This could be due to the fact that samples 1 and 2 were collected from the traffic areas in Bangkok (the capital city of Thailand), whereas sample locations 3-5 were near the power plant area in Lampang (the northern part of Thailand). This observation indicated that SdFFF could be a useful tool for classifying the group of air particulate samples. In this manuscript, size distributions of only five samples are presented. It was not the intention to interpret anything further, but only to demonstrate that SdFFF can be used to give detailed information about particle size in sub-micrometer and micrometer ranges.

Size-based elemental distribution of air particulates

To examine size-based elemental distribution of air particles, the combined technique of SdFFF and ICP-OES was used. As the amount of air particulate samples introduced into the SdFFF channel was very low (i.e., < 0.05 mg) and a very large dilution (> 500-fold) occurred during fractionation, a very sensitive analytical detection technique was needed. With a cross flow nebulizer (CFN), signal intensities of elements were almost not detectable, as shown in Figure 5. To improve the signal intensities of analyte elements, an ultrasonic nebulizer (USN) was therefore used. Signal intensities of Al and Fe in air particulate sample obtained with the CFN compared with those obtained with the USN are shown in Figure 5. The results show that signal intensities of elements in air particulate were increased approximately 5-fold using USN.

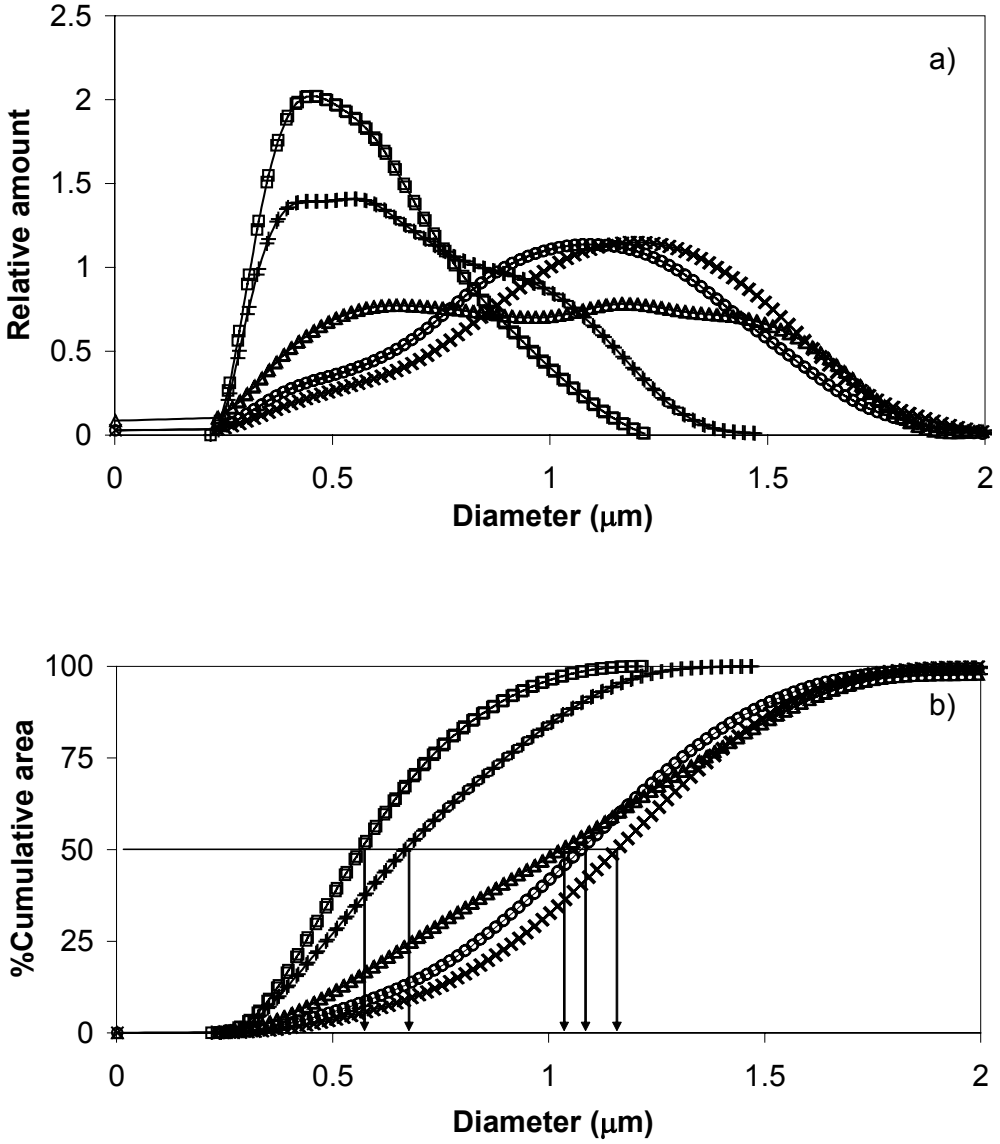

Figure 4 a) Particle size distributions of air particulate samples collected from different locations: location 1 (□), location 2 (+), location 3 (△), location 4 (○), and location 5 (×); and b) the corresponding cumulative plots. The mean diameter values of particulate samples collected from different locations are indicated by the arrows.

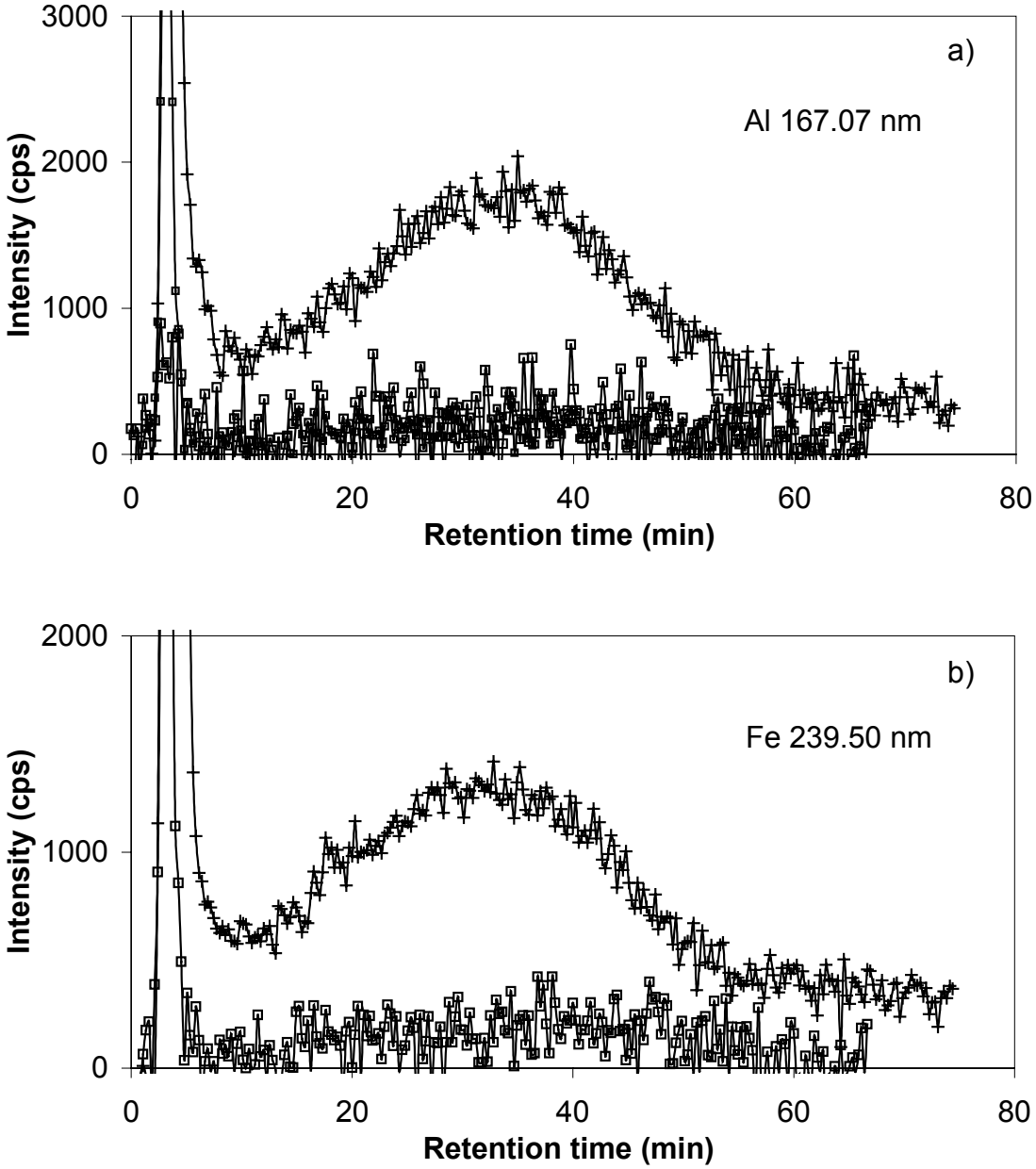

Figure 5 Elemental fractograms of air particulate obtained by SdFFF-ICP-OES with a cross flow (□) and an ultrasonic (+) nebulization for: a) Al; and b) Fe.

The elemental fractograms of an air particulate sample and the corresponding cumulative plots are shown in Figure 6. Broad size distributions were observed for Al, Fe, and Ti with the mean diameters of approximately 1 μm, whereas narrower distribution profile was observed for Mg with the mean diameter of approximately 0.2 μm. Magnesium co-eluted with the void, implying that Mg might be originally present in small size fractions of air particulate or it might be readily dissolved from the suspended air particulate. This observation suggested that Mg was more labile than other elements studied herein. Size distribution profiles of Al, Fe, and Ti (Figure 6b) were correlated well with the distribution profile of air particulate (Figure 6a), suggesting that Al, Fe, and Ti were associated with all size fractions of air particulate sample. This could be due to the fact that Al, Fe, and Ti are major elements in the earth crust, from where most dusts are derived.

One might argue that particle size of air particulate matters in air and in a dispersing medium might be different, and therefore SdFFF might not be suitable for size determination of air particulate matters. Changes in size-based elemental distribution of air particulate matters in different media, i.e., air and dispersing liquid, need further investigation.

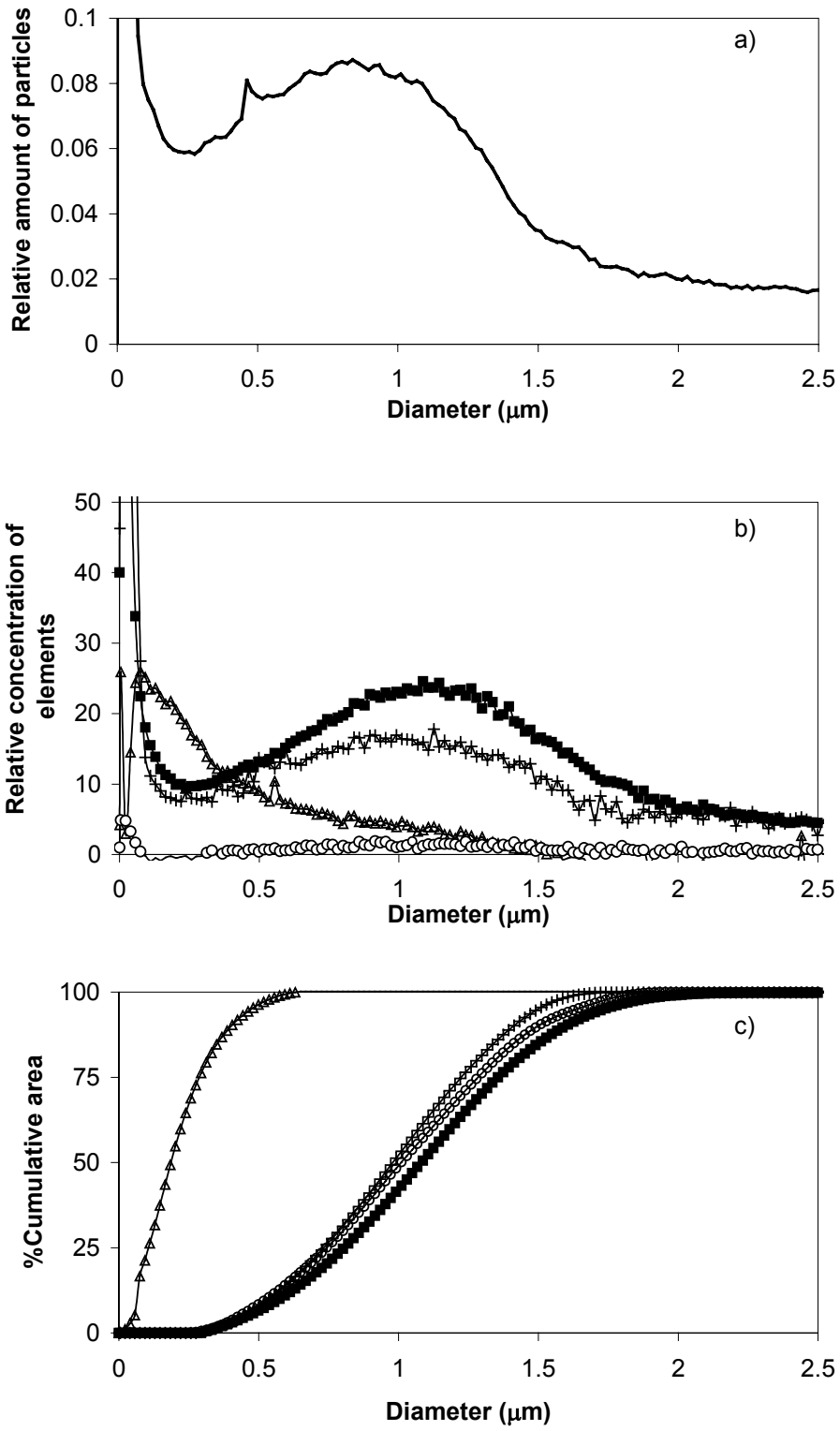

Figure 6 a) Size distribution of air particulate; b) size-based elemental distributions of air particulate, i.e., Al (■), Fe (+), Mg (△), and Si (○); and c) the corresponding cumulative plots.

Conclusions

Details of particle size information and distribution ranges in sub-micrometer and micrometer regions can be obtained using SdFFF technique. To get reliable size information by SdFFF, a proper dispersing agent and carrier liquid must be used to prevent flocculation of suspended particulates. With the use of ICP-OES as the element detector for the fractionated air particulates, the information about size-based elemental distribution of major elements in air particulates could be obtained. It is anticipated that size-based elemental distribution of minor and trace elements in air particulates could be obtained by SdFFF-ICP-MS and the information could be useful in identifying source of pollution. Moreover, size-based elemental speciation would be valuable for predicting the effects of metals on human health and environment. The ultrafine particles are more soluble than the larger size particles. Therefore, the toxicity and potential inflammation on respiratory tract of each element can be predicted using the combined SdFFF with ICP spectrometric detections, either OES or MS.

References

1. Espinosa, A.J.; Rodrigues, M.; Barragan dela Rosa, F.J.; Sanchez, J.C. *Atmos. Environ.*, **2001**, *35*, 2595-2601.
2. Trijonis, J. *Atmos. Environ.*, **1983**, *17*, 999-1008.
3. Mitra, A.P.; Morawska, L.; Sharma, C.; Zhang, J. *Chemosphere*, **2002**, *49*, 903-922.
4. Cormac, B.M. *Introduction to The Scientific Study of Atmospheric Pollution*, Reidel, Dordrecht, Holland, 1997.
5. Kim, W.S.; Kim, S.H.; Lee, D.W.; Lee, S.; Lim, C.S.; Ryu, J.H. *Environ. Sci. Technol.*, **2001**, *35*, 1005-1012.
6. Kim, W.S.; Park, M.; Lee, D.W.; Moon, M.H.; Kim, H.; Lee, S. *Anal. Bioanal. Chem.*, **2004**, *378*, 746-752.
7. Kim, W.S.; Park, Y.H.; Shin, J.Y.; Lee, D.W.; Lee, W. *Anal. Chem.* **1999**, *71*, 3265-3272.

8. Lee, J.Y.; Lee, S.; Min, Y.H.; Hyun, D.Y. *Bull. Korean Chem. Soc*., **2003**, *24*, 1172-1176.
9. Metreau, J.M.; Gallet, S.; Carbot, P.J.P.; Lemairo, V.; Dumus, F.; Hernvann, A.; Loric, S. *Anal. Biochem*., **1997**, *25*1, 178-186.
10. Mezersky, S.M.; Caldwell, K.D.; Jones, S.B.; Mabell, B.E.; Barford, R.A. *Anal. Biochem*., **1988**, *172*, 113-123.
11. Murphy, D.M.; Garbarino, J.R.; Taylor, H.E.; Hart, B.T.; Beckett, R. *J. Chromatogr*., **1993**, *642*:459-467.
12. Barman, B.N.; Giddings, J.C. *Polym. Mater. Sci. Eng*., **1990**, *62*, 186-190.
13. Ranville, J.F.; Chiltleborough, D.J.; Shanks, F.; Morrison, J.S.; Harris, T.; Doss, F.; Beckett, R. *Anal. Chim. Acta*, **1999**, *381*, 315-329.
14. Kim, W.S.; Lee, D.W. *Anal. Chem*., **2002**, *74*, 848-855.
15. Park, Y.H.; Kim, W.S.; Lee, D.W. *Anal. Bioanal. Chem*., **2003**, *375*, 489-495.
16. Allen, A.G.; Nemitz, E.; Shi, J.P.; Harrision, R.M.; Greenwood, J.C. *Atmos. Environ*., **2002**, *35*, 4851-4592.
17. Chow, J.; Watson, J.; Fujita, E.; Lu, Z.; Lawson, D.; Ashbaugh, L. *Atmos. Environ*., **1994**, *28*, 2061-2080.
18. Rodriguez, S.; Querol, X.; Alastuey, A.; Viana, M.; Alarcoh, M.; Mantilla, E. *Sci. Total Environ*., **2004**, *328*, 95-113.
19. Ondov, J.M.; Zoller, W.H.; Gordon, G.E. *Environ. Sci. Technol*., **1982**, *16*, 318-328.
20. Natusch, D.F.S.; Wallace, J.R.; Evans, C.A. *Science*, **1974**, *183*, 202-204.
21. Beckett, R.; Nicholson, G.; Hart, B.T.; Hansen, M.; Giddings, J.C. *Water Res*., **1988**, *22*, 1535-1545.
22. Dondi, F.; Martin, M. In Schimpf ME, Caldwell JC, Giddings JC (eds) *Field-Flow Fractionation Handbook*, Wiley, New York, 2000, pp 103-132.
23. Giddings, J.C.; Moon, M.H.; Williams, P.S.; Myers, M.N. *Anal. Chem*., **1991**, *63*, 1366-1372.
24. Mari, Y.; Scarlett, B.; Merkus, H.G. *J. Chromatogr*., **1990**, *515*, 27-35.

บทที่ 2

Field-flow fractionation-inductively coupled plasma mass spectrometry: an alternative approach to investigate metal-humic substances interaction

Abstract

Interaction between metal ions and humic matter was investigated using a hyphenated technique, field-flow fractionation-inductively coupled plasma mass spectrometry (FFF-ICP-MS). Aggregation of a metal-spiked commercial Aldrich humic acid in an aqueous solution of calcium ion or in seawater was examined over time intervals of 0 min to 4,320 min. The aggregation was demonstrated by shifts in peak maximum of humic matter from smaller size (2.9 nm) to larger size (5.1 or 5.8 nm in Ca^{2+} solution or in seawater, respectively), and also by the broadening of size distribution profiles. With FFF, size distribution of humic aggregate was characterized. Further, dominant particle size (2.9 nm), mean particle size (3.8 nm), and diffusion coefficient (1.51×10^{-6} cm^2/s) of humic acid solution were determined. With FFF-ICP-MS, associations of Cd, Cu, and Pb with humic aggregates were examined. The mean diameters of Cd-, Cu-, and Pb-bound humic aggregates in the metal-spiked humic acid were 4.1, 4.5, and 5.8 nm, respectively. These diameters were shifted to 6.0, 6.0, and 6.9 nm, respectively, in the humic acid incubated with calcium solution, whereas they were shifted to 6.5, 5.7, and 7.4 nm, respectively, in the humic acid incubated with seawater for 3 days. Humic aggregate of small size showed more affinity for Cu than Cd and Pb, whereas the large aggregate showed more affinity for Pb than Cd and Cu, respectively.

Introduction

Understanding the humic substances is one of the central issues of environmental studies, since they play vital roles in the regulation of nutrient and toxic elements in terrestrial and aquatic environments [1,2]. Humic acids are thought to either be associations of relatively small molecules held together [3] or polymers exhibiting random coil conformation [4]. Although the exact structure of humic acid is still controversial, it is reported to be very sensitive to pH and ionic strength changes [5-7]. Only slight alterations in pH or ionic strength affect the structural conformation of humic macromolecules, and sometimes lead to humic aggregation [5, 8-11] or flocculation [12]. Detailed knowledge about humic

aggregation phenomenon is still lacking. To investigate the aggregation, a reliable size separation technique is required. An overview of structural and size characterization method for humic substances was recently given [13]. Numerous advanced analytical and separation techniques including vapor-pressure osmometry, high pressure size exclusion chromatography (HP-SEC) [14-17], capillary zone electrophoresis (CZE) [18,19], polyacrylamide gel electrophoresis (PAGE), analytical centrifugation, light scattering, mass spectrometry, and flow field-flow fractionation (FlFFF) [10,11,20,21] have been reported for size characterization of humic materials. Nonetheless, discrepancies among methods were observed, because of the measurement artifacts. Thus, puzzles of exact humic structure and size still remain to be solved. Among size separation techniques, HP-SEC is the most commonly used approach. However, the potential interactions among humic acids with a stationary phase restrict the use of HP-SEC.

In this study, a FlFFF was employed for size characterization of humic acid. Although good agreement between the humic acid size data obtained from FlFFF and HP-SEC was demonstrated [22], the opportunity for humic molecules adsorption and degradation was minimized with the open channel characteristic (reduced surface area) of FlFFF in comparison with the packed HP-SEC column [20]. With FlFFF, various information on physicochemical properties of humic aggregate, i.e., diameter, size distribution, diffusion coefficient, can be obtained. The purpose of this study is to investigate the aggregation of humic acid both in Ca^{2+} solution and in seawater. Further, an ICP-MS was used as element detector after humic size separation by FlFFF, in order to investigate size distributions of Cd, Cu, and Pb binding humic acid aggregate. In addition, shifts in metal ions size distributions in the humic aggregates incubated in Ca^{2+} solution and seawater were observed, in order to examine how these metal ions changed with humic aggregate size. A number of literatures on FFF-ICP-MS [23-29] have appeared since the technique was first proposed in 1991 [30] with the first experimental results reported in 1992 [31]. Nonetheless, this study shows a novel application of FFF-ICP-MS, and also suggests that the FFF-ICP-MS is an essential tool for characterization of metal-humic interaction.

Experimental

Chemicals and molecular weight standards

A stock solution of 4,000 mg/L Ca was prepared by dissolving 0.147 g of analytical reagent grade $CaCl_2 \cdot 2H_2O$ (Fisher Scientific Co., Fair Lawn, NJ, USA) in 10 mL of deionized water. Stock solutions of 100 mg/L Cd, Cu, and Pb were made by dissolving 0.0210, 0.0297, and 0.0207 g of $Cd(NO_3)_2$, $Cu(NO_3)_2$, and $Pb(NO_3)_2$ (Merck, Darmstadt, Germany) in 100 mL deionized water. A 30 mM TRIS buffer was prepared by dissolving 3.6 g of tris (hydroxymethyl aminomethane) (Fisher Scientific Ltd., Leicestershire, U.K.) in deionized water 1,000 mL and titrating to pH 7.5 with concentrated nitric acid.

Poly(styrene sulfonic acid sodium salt) molecular weight standards (1.4, 4.4, 15.2, and 43.3 kDa, Fluka Chemie GmbH., Switzerland) were used to calibrate the FlFFF channel. All standards were dissolved in 30 mM TRIS at pH 7.5.

Metal spiked humic acid

A commercial humic acid from an open pit mining area in Germany, purchased from Aldrich (Steinheim, Germany), was used in this study. The assays of the Aldrich humic acid are as follow: 39.0%C; 4.4%H; 3%S; 2%Na; 1.4%Fe; 0.5%Ca; 0.4%N; 0.4%Al; 0.05%Mg; and 0.04%K. A humic acid stock solution (6,000 mg/L) was made by dissolving 0.060 g of the Aldrich humic acid in 10 mL of deionized water. A metal spiked humic acid was prepared by mixing 5 mL of the dissolved Aldrich humic acid with the metal ion solutions, and then making up to 10 mL with deionized water to contain 2, 6, and 2 mg/L of Cd, Cu, and Pb, respectively. This solution is hereafter referred to as “spiked humic acid”. To study aggregation behavior of the spiked humic acid in the presence of Ca^{2+}, a 500 μL aliquot of humic acid solution was mixed with 400 μL of Ca^{2+} solution, and made up with deionized water to obtain final humic acid concentration of 2,000 mg/L, and Ca^{2+} concentration of 1,600 mg/L. To study aggregation behavior of the spiked humic acid in seawater, a 500 μL aliquot of spiked humic acid solution was mixed with seawater collected from the Jomtien Beach (Pattaya, Thailand) to obtain final humic acid concentration of 2,000 mg/L.

Instrumentation

A FlFFF system (Model PN-1021-FO, Postnova Analytik, Germany) equipped with a 1 kDa molecular weight cut-off, regenerated cellulose acetate membrane (Postnova) was used. The FlFFF channel was 27.7 cm long, 2.0 cm wide, and 254 μm thick. The humic acid sample was injected directly into an injector valve (Rheodyne) with a fixed loop (20 μL) attached to the FlFFF channel front end. A 30 mM TRIS buffer (pH 7.5) was used as a carrier liquid throughout this study. An HPLC pump (Model PN 2101, Postnova Analytik, Germany) delivered the channel flow at 1 mL/min. Another HPLC pump of the same model was employed to regulate the cross flow rate at 2 mL/min. A relaxation time of 2 min was allowed for sample particles situated at the top wall to move to the accumulation wall. The UV detector (UV-2000 Spectra SYSTEM) was set at 254 nm to monitor light attenuation of separated humic acid samples. An ICP-MS (Sciex/Elan 6000, PerkinElmer Instruments, Shelton, CT) was used as an element detector after the UV absorption detector as illustrated in Figure 1. Owing to the similarity of the FlFFF channel flow and ICP-MS sampling flow rates typically used for analysis, the ICP-MS cross-flow nebulizer was connected directly to the UV detector outlet with a 35-cm length of poly(tetrafluoroethylene) tubing (PTFE, 0.58 mm id). The FIFFF-ICP-MS operating conditions are summarized in Table 1.

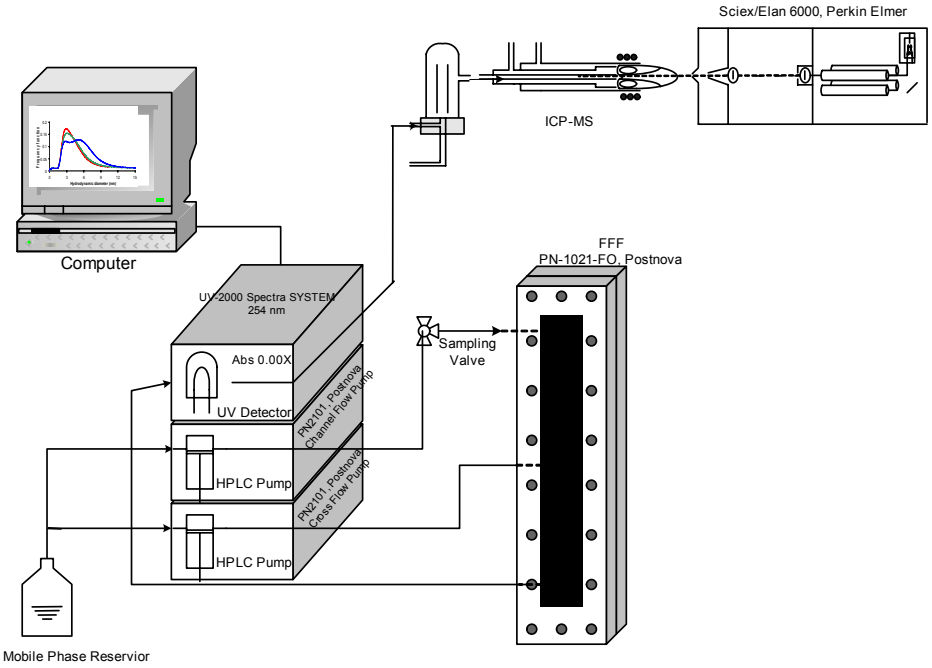

Figure 1 Schematic diagram illustrating FlFFF-ICP-MS arrangement.

Table 1 FIFFF-ICP-MS operating conditions

Flow FFF Model PN-1021-FO	
FFF channel dimensions (cm)	27.7 long x 2.0 wide x 0.02 cm thick
Carrier liquid	30mM TRIS (buffered at pH 7.5)
Channel flow rate (mL/min)	1.0
Cross flow rate (mL/min)	2.0
Equilibration time (min)	2.0
Membrane	1 kDa MWCO poly(regenerated cellulose acetate)
ICP-MS Elan 6000	
Rf generator frequency (MHz)	40
Rf forward power (W)	1000
Torch	Fassel type
Torch injector	Ceramic alumina
Spray chamber	Ryton® Scott double pass
Nebulizer	Gem-tip® cross flow
Nebulizer gas flow rate (L/min)	0.95
Intermediate gas flow rate (L/min)	1.2
Outer gas flow rate (L/min)	15
Resolution	1 ± 0.1 at 10% peak maximum
Scanning mode	Peak hop transient signal
Measurement per peak	1
Dwell time (ms)	200
Isotopes monitored (m/z)	^{63}Cu, ^{65}Cu, ^{111}Cd, ^{114}Cd, ^{206}Pb, ^{208}Pb

Observation of humic acid aggregation

The aggregation at room temperature was observed immediately after mixing calcium ion solution, or seawater with humic solutions. Recording of data was performed at appropriate intervals of 1, 60, 180, 300, and 4,320 min.

Data transformation

Raw fractograms were translated into size distribution profiles using an Excel (Microsoft® Excel 2002, Redmond, WA) spreadsheet. Peak area normalization, and cumulative area determination were performed using PeakFit™ (SPSS, Chicago, IL, USA).

Results and discussions

Particle size characteristics: evidence on humic aggregation

To obtain the information about hydrodynamic size of humic acid, retention times (t_r) of a raw fractogram were translated into hydrodynamic diameters (d_h). Consequently, the raw fractograms were converted into the hydrodynamic size distributions using the method described by Beckett et al. [32] and Schimpf et al. [33]. Once the size distribution profile was plotted, particle size at peak maximum (d_p), breadth of size distributions ($\Delta d_{0.5}$), and mean particle size (d_{mean}) were measured.

Particle size at peak maximum (d_p) was used to identify the dominant particle size of the investigated humic acid. To quantify the breadth of size distributions, particle size ranges at half maximum height ($\Delta d_{0.5}$) were calculated from the distribution profiles. The measured d_p and $\Delta d_{0.5}$ values for humic aggregates in Ca^{2+} solution and in seawater at various contact times are summarized in Table 2. To obtain the mean particle size (d_{mean}) of humic aggregates, the diameter distribution profiles (Figure 2) were converted into cumulative area plots as shown in Figure 3. The d_{mean} is defined as the particle size at which

50% of the total accumulative area is detected. The d_{mean} values were determined from the cumulative plots, as summarized in Table 2. To illustrate the measurement precision, size characterization of humic acid without addition of Ca^{2+} or seawater was performed 9 times and the results are as follow: d_p = 2.90 $\pm$ 0.05; d_{mean} = 3.80 $\pm$ 0.03; and $\Delta d_{0.5}$ = 3.10 $\pm$ 0.08.

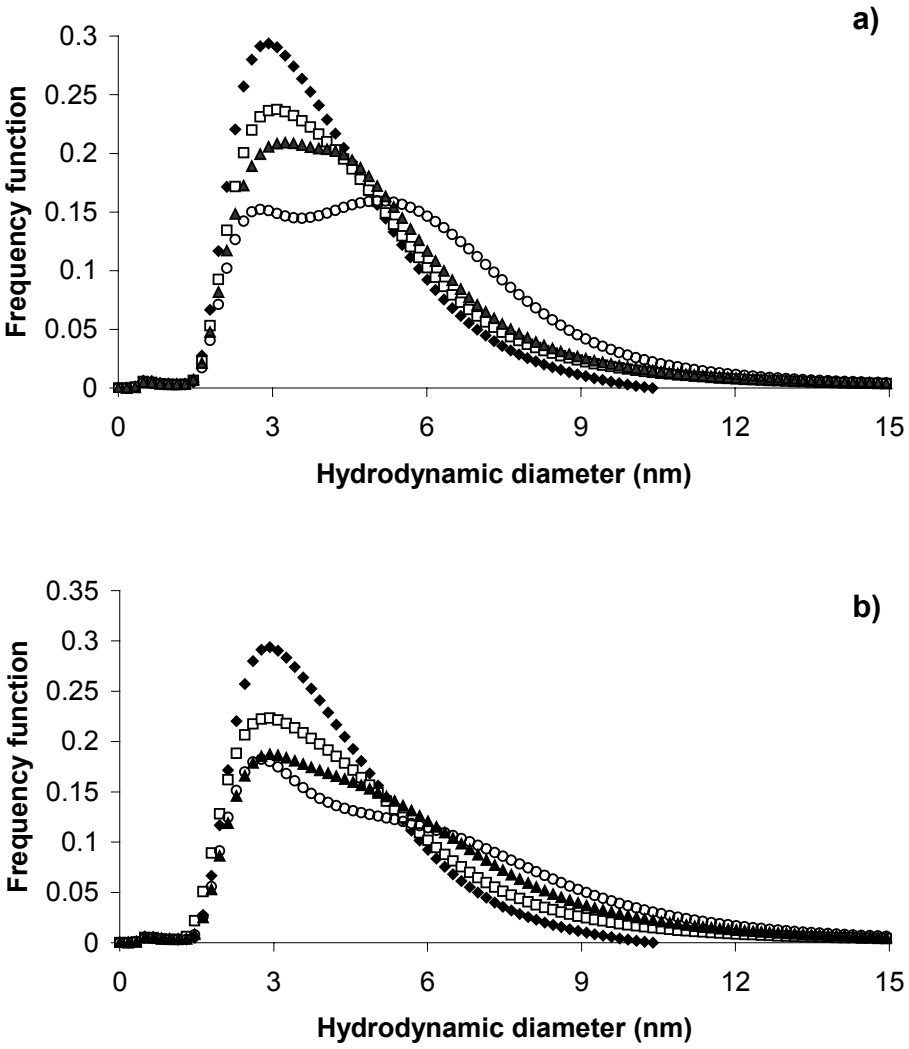

Figure 2 Hydrodynamic diameter distributions of humic acid (2,000 mg/L) in: (a) Ca^{2+} 1,600 mg/L; and (b) seawater; at 0 min (◆), 60 min (□), 180 min (▲), and 4,320 min (○) contact time. (Owing to the similarity between the hydrodynamic diameter distributions of humic acids at 180 and 300 min contact times, hydrodynamic diameter distribution of humic acid at 300 min contact time is not shown.)

In this study, particle size information obtained from FlFFF is used to provide evidence on humic aggregation. The aggregation phenomenon of humic acid (2,000 mg/L) in the presence of Ca^{2+}(1,600 mg/L) was temporally investigated as demonstrated by shifts in size distributions with increasing contact time (Figure 2a). With increasing contact time between humic acid and Ca^{2+}, the size distributions slightly broadened, and yielded a bimodal size distribution characteristic at extended contact time (4,320 min). The peak maxima appeared at longer retention times or at larger diameter sizes (Figure 2a and Table 2), providing a clear evidence of humic aggregation. Particle size at peak maximum (d_p), mean particle size (d_{mean}), and breadth of size distributions ($\Delta d_{0.5}$) increased with increasing contact time, suggesting that the aggregation process gradually took place. In seawater, however, d_{mean} and $\Delta d_{0.5}$ increased, whereas the d_p remained constant with increasing contact time. This finding suggests that in order to observe humic acid aggregation, information on particle size at peak maximum (d_p) only is not adequate. The d_{mean} and $\Delta d_{0.5}$ also should be considered. In seawater medium, the bimodal characteristic was initially observed at contact time of 180 min (Figure 2b). At 180-min contact time, the dominant hydrodynamic sizes were observed at 2.9 and 5.2 nm. The former remained constant and the latter increased with increasing contact time. These could suggest that aggregation only occurred with humic matter of larger sizes.

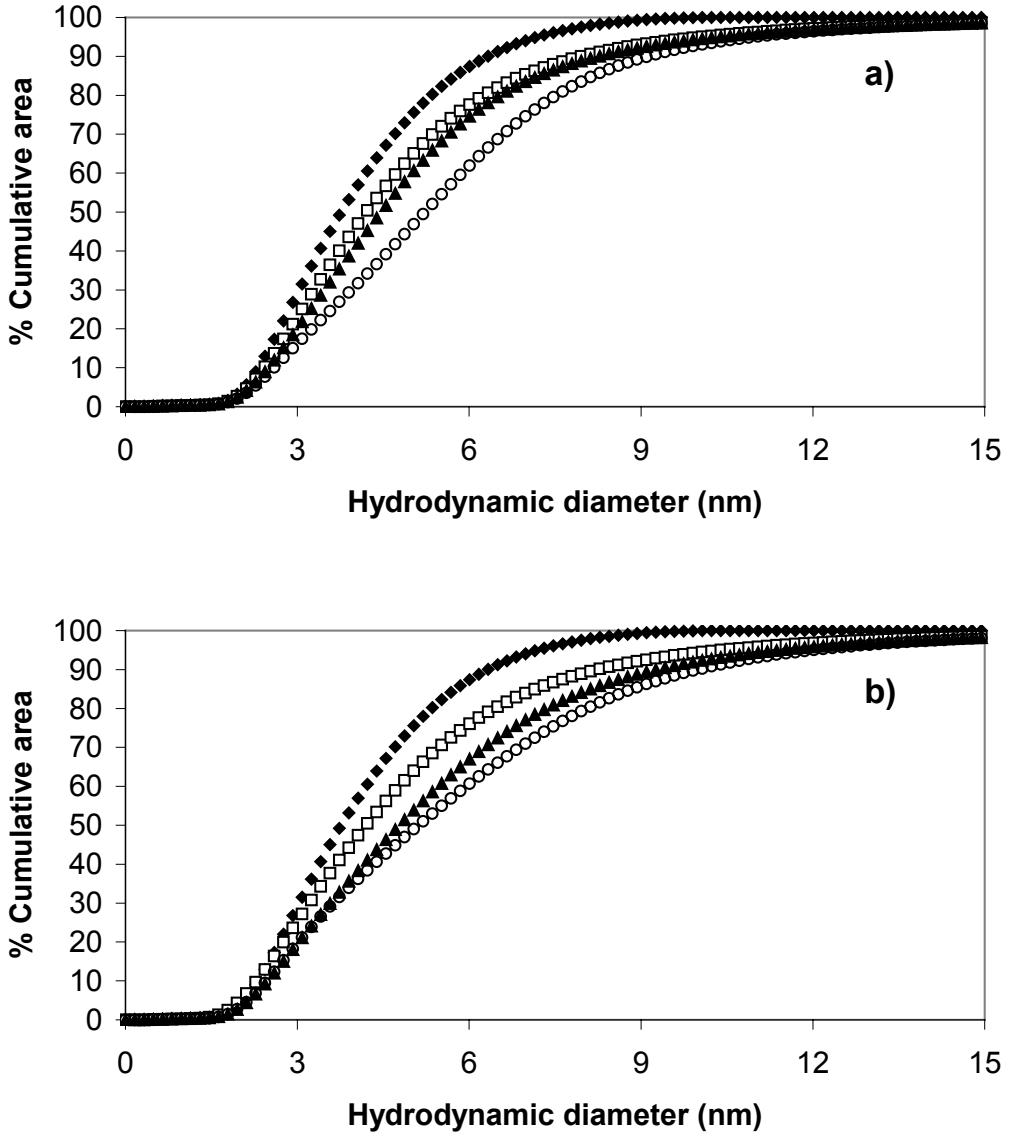

Figure 3 Cumulative area plots for humic acid (2,000 mg/L) in: (a) Ca^{2+} 1,600 mg/L; and (b) seawater; at 0 min (◆), 60 min (□), 180 min (▲), and 4,320 min (○) contact time. (Owing to the similarity between the cumulative area plots for humic acids at 180 and 300 min contact times, cumulative area plot for humic acid at 300 min contact time is not shown.)

Table 2 Particle size information of humic aggregate

contact time	diameter of humic aggregate in Ca^{2+} solution (nm)		
(min)	d_p	d_{mean}	$\Delta d_{0.5}$
0	2.9	3.8	3.1
60	3.1	4.2	3.7
180	3.3	4.5	4.2
300	3.6	4.6	4.5
4,320	2.8 and 5.1	5.2	5.8
contact time	diameter of humic aggregate in seawater (nm)		
(min)	d_p	d_{mean}	$\Delta d_{0.5}$
0	2.9	3.8	3.1
60	2.9	4.2	3.9
180	2.9 and 5.2	4.8	4.8
300	2.8 and 5.4	4.9	5.1
4,320	2.8 and 5.8	5.1	5.3

Diffusion coefficients of humic aggregate

Flow field-flow fractionation also provides information on diffusion properties of humic acid [10,20]. Diffusion coefficient of humic aggregate is an inverse function of hydrodynamic diameter as follows: $D = kT/3\pi\eta d_h$; where k is the Boltzmann's constant (1.38×10^{-16} g $cm^2/s^2\ K^1$), T is absolute temperature (K), and η is the carrier liquid viscosity (g/cm s). In this study, diffusion coefficient at peak (D_p) and mean diffusion coefficient (D_{mean}) of humic aggregates were computed as summarized in Table 3. Distribution of diffusion coefficient also was plotted as illustrated in Figure 4. The experimentally obtained values of D_p are in the same order of magnitude as what reported by other investigators [20]. Particles or macromolecules of larger size exhibit less diffusion coefficients than the smaller counterparts. In Ca^{2+} solution, D_{mean} decreased with increasing contact time, implying that the humic aggregate became less mobile in the presence of calcium ion. Furthermore, the ratio between D_{mean} and D_p is proposed here to describe the degree of normal distribution. A ratio of 1 indicates a symmetrical normal distribution profile, whereas a ratio deviating from 1 suggests the presence of distribution asymmetry. The D_{mean}/D_p of humic aggregate at contact times up to 3 hours were close to unity, indicating normal distribution profiles of the diffusion coefficient values. Nonetheless, the ratios deviated from unity with increasing contact time, suggesting that the diffusion coefficient values deviated from normal distribution as the larger aggregates were gradually formed.

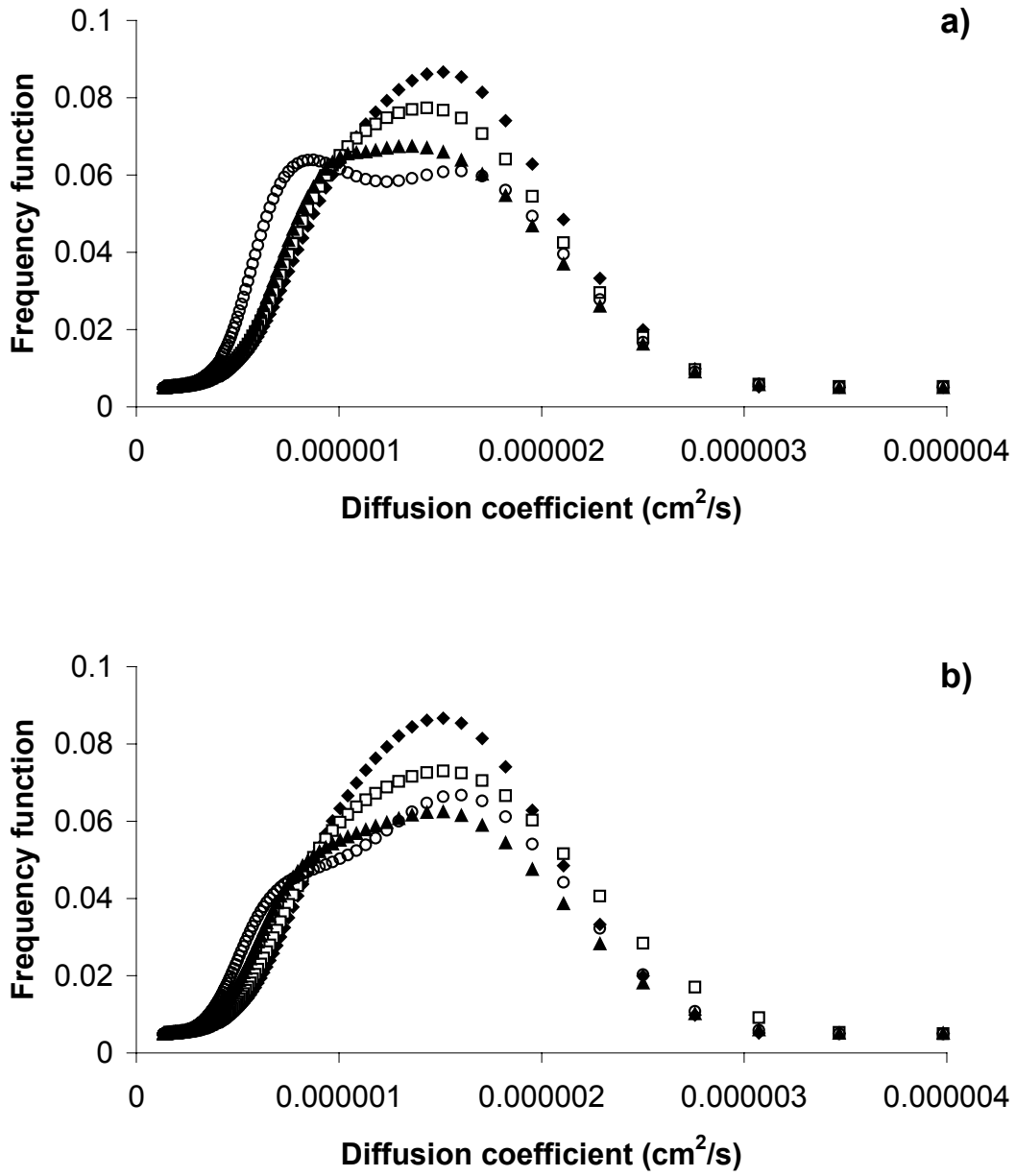

Figure 4 Diffusion coefficient distributions of humic acid (2,000 mg/L) in: (a) Ca^{2+} 1,600 mg/L; and (b) seawater; at 0 min (◆), 60 min (□), 180 min (▲), and 4,320 min (○) contact time. (Owing to the similarity between the diffusion coefficient distributions of humic acids at 180 and 300 min contact times, diffusion coefficient distribution of humic acid at 300 min contact time is not shown.)

Size distributions of metal ions-bound humic acid

Association of metal ions with humic aggregates was observed using FlFFF-ICP-MS. The ion fractograms of Cd, Cu, and Pb were obtained by ICP-MS detection after size separation of humic aggregates by FlFFF. The ion fractograms were then translated into hydrodynamic size distributions. The normalized size distributions of Cd-, Cu-, and Pb-bound humic aggregates in Ca^{2+} solution or seawater are shown in Figures 5-6, respectively. Once the elemental profile showing size distribution of metal ions-bound humic aggregates was plotted, particle size at peak maximum (d_p), breadth of size distributions ($\Delta d_{0.5}$), and mean particle size (d_{mean}) of each metal ions were measured, as summarized in Table 4. In both Ca^{2+} solution and seawater, the d_p, d_{mean}, and $\Delta d_{0.5}$ of Pb-bound humic aggregates were larger than those of Cd and those of Cu. The findings, in which the d_p and d_{mean} of Pb-bound humic aggregates were largest, suggest that large humic aggregate has more affinity for Pb than Cd and Cu, whereas small humic aggregate has more affinity for Cu than Cd and Pb. The $\Delta d_{0.5}$ value of Pb-bound humic aggregates was largest, implying that the hydrodynamic sizes of Pb were more dispersed in comparison with those of Cd and Cu. For a closer look of the $\Delta d_{0.5}$ values, Cd- and Cu-bound humic aggregates exhibited same degree of size distribution breadth for the spiked humic acid (without addition of Ca^{2+} or seawater) and the spiked humic acid in both Ca^{2+} solution and seawater at extended contact time (4,320 min). However, the size distributions of Cu-bound humic aggregates were narrower than those of Cd at contact times of less than 5 hours. These suggest that the hydrodynamic sizes of Cu-bound humic aggregates were less dispersed than those of Cd. At extended contact time, broader size distributions of all metal ions-bound humic aggregates were observed in seawater as compared to in Ca^{2+} solution. This is especially true for Pb-bound humic aggregates, whose size distribution breadth equals 6.6 or 8.7 in Ca^{2+} solution or in seawater, respectively. Therefore, a conclusion is made that all metal ions-bound humic aggregates were dimensionally more dispersed in seawater than in Ca^{2+} solution.

To examine how metal ions are distributed in each humic size fractions, size distribution profiles of humic acid, and Cd-, Cu-, and Pb-bound humic aggregates were plotted together, as illustrated in Figure 7. In the spiked humic acid, Cd- and Cu-bound

humic acid size distributions followed humic size distribution quite well with a slight shift in peak maxima (d_p of humic, Cd, and Cu were 2.9, 4.0, and 3.7 nm, respectively), whereas Pb-bound humic aggregates shows broader size range with a significant shift in peak maximum (d_p of Pb-bound humic acid was 4.6 nm, see Figure 7a). These are the evidences that metal ions have the preference to associate with larger humic aggregates than the smaller counterparts.

Table 3 Diffusion coefficients of humic aggregate

contact time	in Ca^{2+} solution		
(min)	D_p	D_{mean}	D_{mean} / D_p
0	1.51×10^{-6}	1.51×10^{-6}	1
60	1.43×10^{-6}	1.47×10^{-6}	1.03
180	1.34×10^{-6}	1.41×10^{-6}	1.05
300	1.22×10^{-6}	1.41×10^{-6}	1.16
4,320	0.87×10^{-6}	1.40×10^{-6}	1.61
contact time	in seawater		
(min)	D_p	D_{mean}	D_{mean} / D_p
0	1.51×10^{-6}	1.51×10^{-6}	1
60	1.51×10^{-6}	1.56×10^{-6}	1.03
180	1.49×10^{-6}	1.45×10^{-6}	0.97
300	1.56×10^{-6}	1.47×10^{-6}	0.94
4,320	1.58×10^{-6}	1.51×10^{-6}	0.96

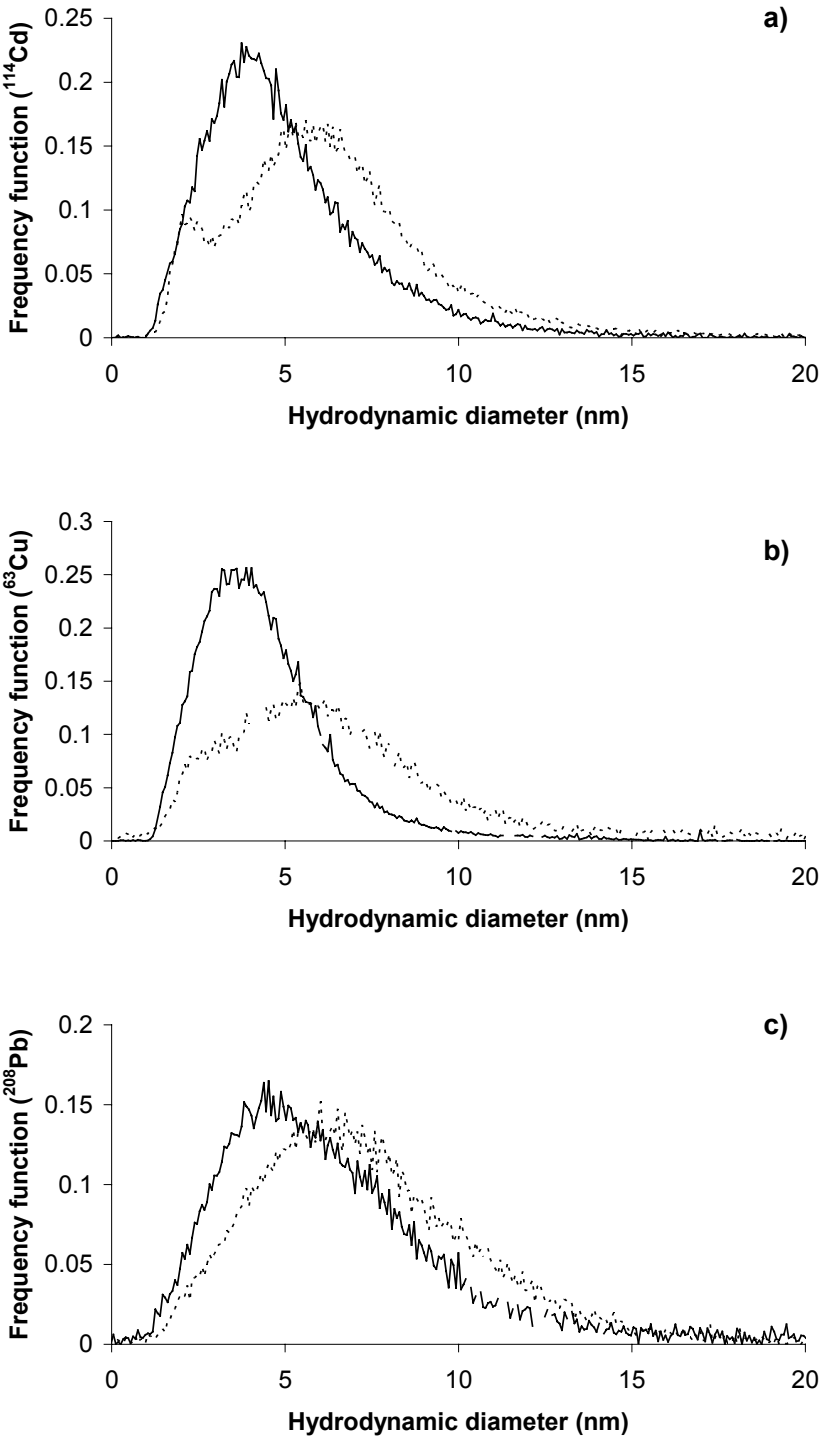

Figure 5 Hydrodynamic diameter distributions of: (a) ^{114}Cd-; (b) ^{63}Cu-; and (c) ^{208}Pb-; bound humic aggregates in the spiked humic acid (——) and spiked humic acid incubated in Ca^{2+} 1,600 mg/L for 4,320 min (- - -).

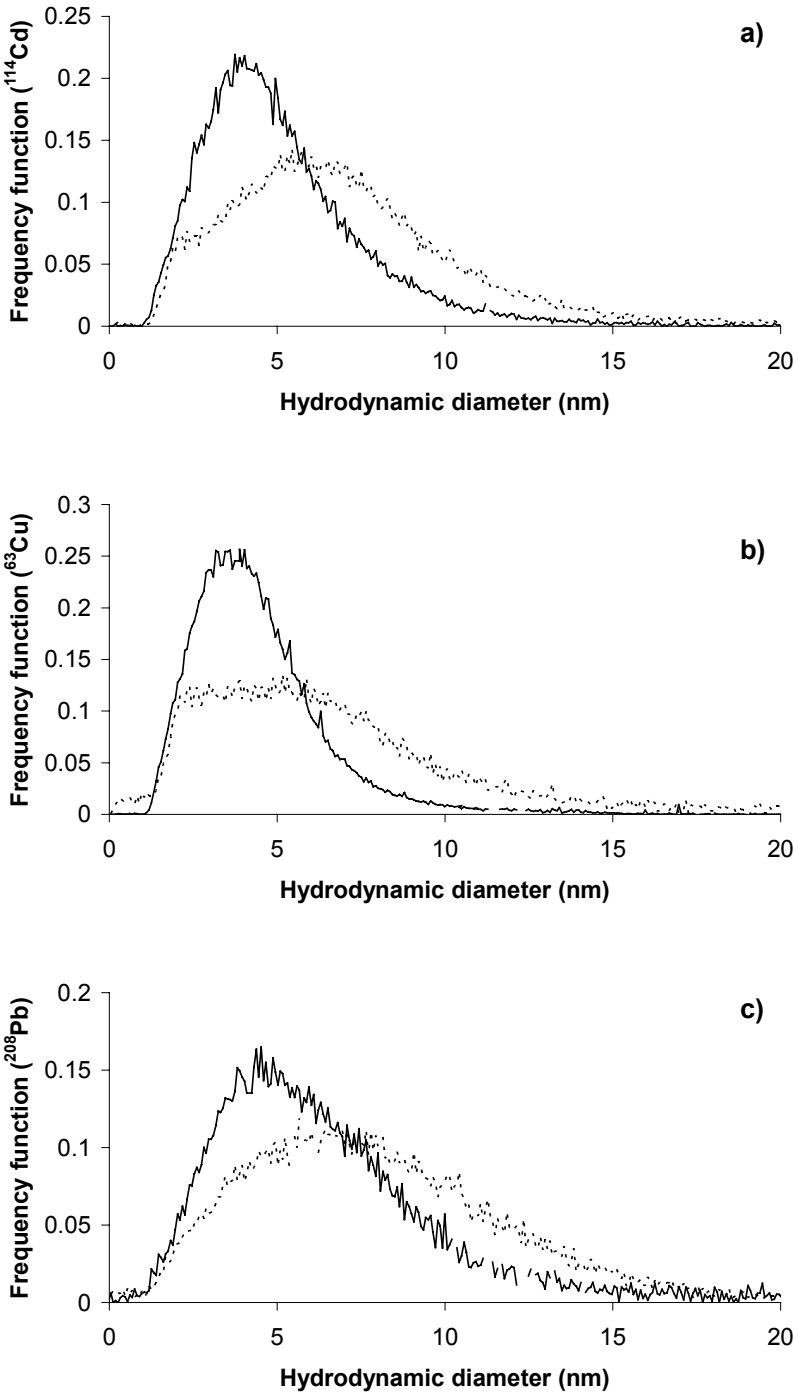

Figure 6 Hydrodynamic diameter distributions of: (a) ^{114}Cd-; (b) ^{63}Cu-; and (c) ^{208}Pb-; bound humic aggregates in the spiked humic acid (——) and spiked humic acid incubated in seawater for 4,320 min (- - -).

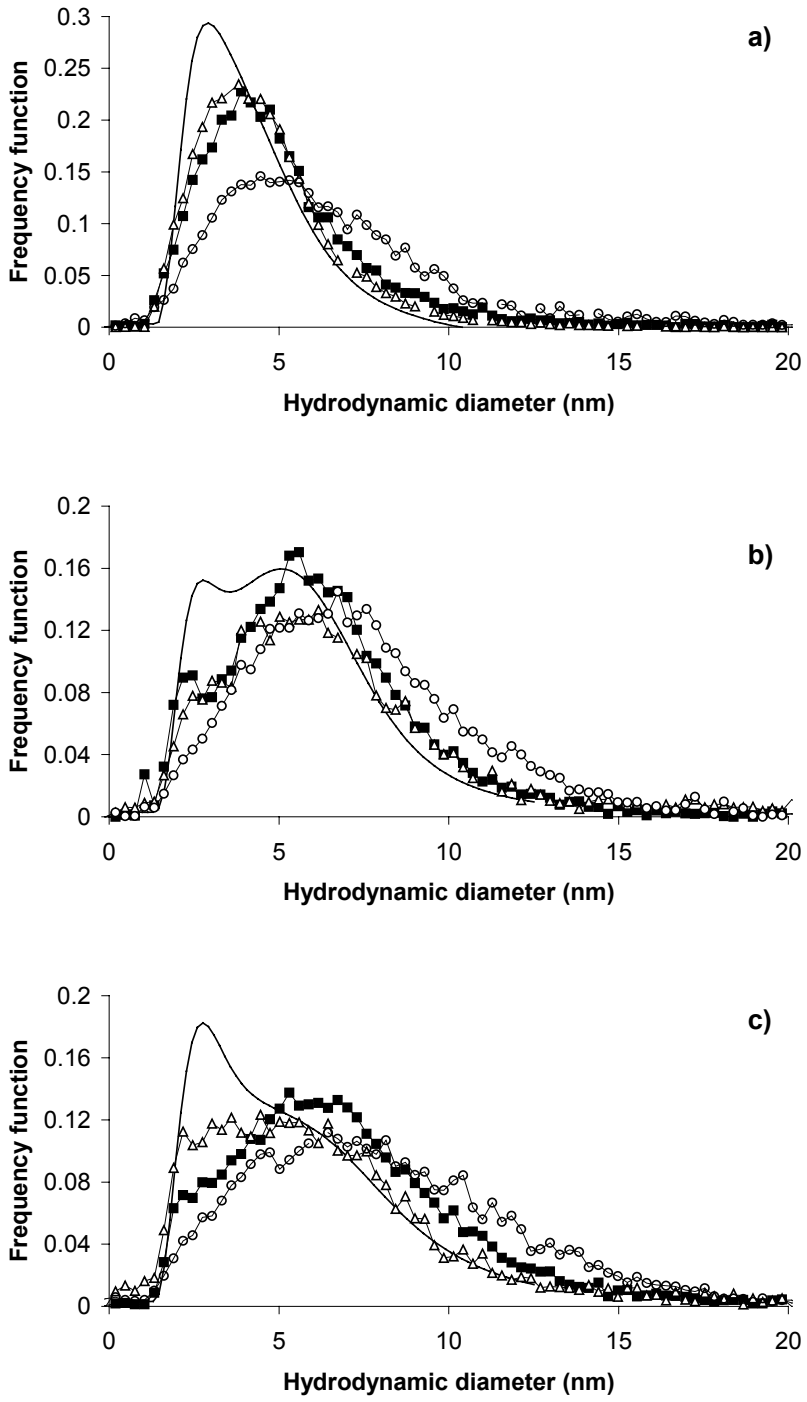

Figure 7 Hydrodynamic diameter distributions of humic acid (—) and the associated metal ions, i.e., ^{114}Cd (■), ^{63}Cu (△), and ^{208}Pb (O): (a) the spiked humic acid; (b) spiked humic acid incubated in Ca^{2+} 1,600 mg/L for 4,320 min; and (c) spiked humic acid incubated in seawater for 4,320 min.

Table 4 Particle size information of metal ions in humic aggregate

contact time	humic aggregate in Ca^{2+} solution								
(min)	$d_{p[Cd]}$	$d_{p[Cu]}$	$d_{p[Pb]}$	$d_{mean[Cd]}$	$d_{mean[Cu]}$	$d_{mean[Pb]}$	$\Delta d_{0.5[Cd]}$	$\Delta d_{0.5[Cu]}$	$\Delta d_{0.5[Pb]}$
0	4.0	3.7	4.6	4.5	4.1	5.8	3.8	3.9	5.4
60	4.5	4.0	5.4	5.1	4.2	6.3	3.9	3.5	6.2
180	4.7	4.3	5.7	5.5	4.7	6.7	4.5	3.6	6.5
300	5.0	4.5	5.9	5.5	4.8	6.8	4.7	3.8	6.9
4,320	5.6	5.5	6.3	6.0	6.0	6.9	6.3	6.3	6.6
contact time	humic aggregate in seawater								
(min)	$d_{p[Cd]}$	$d_{p[Cu]}$	$d_{p[Pb]}$	$d_{mean[Cd]}$	$d_{mean[Cu]}$	$d_{mean[Pb]}$	$\Delta d_{0.5[Cd]}$	$\Delta d_{0.5[Cu]}$	$\Delta d_{0.5[Pb]}$
0	4.0	3.7	4.6	4.5	4.1	5.8	3.8	3.9	5.4
60	4.7	3.9	5.4	5.2	4.4	6.3	4.9	4.0	6.4
180	5.2	4.5	6.6	6.0	5.0	7.2	5.4	4.3	7.5
300	5.5	4.7	6.7	6.1	5.2	7.4	5.6	4.8	7.7
4,320	6.0	4.7	6.6	6.5	5.7	7.4	6.9	6.9	8.7

Notes: $d_{p[Cd]}$, $d_{mean[Cd]}$, or $\Delta d_{0.5[Cd]}$ represents d_p, d_{mean}, or $\Delta d_{0.5}$, respectively, of Cd in humic aggregate

$d_{p[Cu]}$, $d_{mean[Cu]}$, or $\Delta d_{0.5[Cu]}$ represents d_p, d_{mean}, or $\Delta d_{0.5}$, respectively, of Cu in humic aggregate

$d_{p[Pb]}$, $d_{mean[Pb]}$, or $\Delta d_{0.5[Pb]}$ represents d_p, d_{mean}, or $\Delta d_{0.5}$, respectively, of Pb in humic aggregate

Furthermore, the mean diameter ratio between metal ions-bound humic aggregate and humic aggregate was calculated, as summarized in Table 5. This value can be used as an index to predict how metal is distributed across humic size range. The value of 1 indicates that the metal ions are distributed evenly across humic size range and the value higher than 1 suggests that the metal ions are associated more with larger size than the

smaller size aggregate. Conversely, the value less than 1 implies that the metal ions are associated more with smaller size than the larger size aggregate. The mean diameter ratio of Cu was close to unity, suggesting that Cu-bound humic acid size distribution was well correlated with size distribution of humic acid. Size distributions of Pb-bound humic aggregates, however, were less correlated with humic size distribution, as compared to those of Cu and Cd.

Table 5 Mean diameter ratios between metal ion and humic aggregate

contact time	humic aggregate in Ca^{2+} solution		
(min)	$d_{mean[Cd/humic]}$	$d_{mean[Cu/humic]}$	$d_{mean[Pb/humic]}$
0	1.18	1.08	1.53
60	1.21	1.00	1.50
180	1.22	1.04	1.49
300	1.20	1.04	1.48
4,320	1.15	1.15	1.33
contact time	humic aggregate in seawater		
(min)	$d_{mean[Cd/humic]}$	$d_{mean[Cu/humic]}$	$d_{mean[Pb/humic]}$
0	1.18	1.08	1.53
60	1.24	1.05	1.50
180	1.25	1.04	1.50
300	1.24	1.06	1.51
4,320	1.27	1.12	1.45

Notes: $d_{mean[Cd/humic]}$ represents the mean diameter ratio between Cd and humic aggregate

$d_{mean[Cu/humic]}$ represents the mean diameter ratio between Cu and humic aggregate

$d_{mean[Pb/humic]}$ represents the mean diameter ratio between Pb and humic aggregate

Elemental ratios across size distribution

Murphy et al. [23] and Hassellöv et al. [24] suggested that the elemental atomic ratio distributions could be used to follow changes in chemical composition of mixtures as a function of particle size. In Figure 8, the elemental atomic ratios are plotted against hydrodynamic diameters. The Pb/Cd and Pb/Cu for the spiked humic acid (without addition of Ca^{2+} or seawater) were less than 1 in the size range between 2 and 5 nm and were larger than 1 in the hydrodynamic diameters larger than 6 nm. The Pb/Cu was higher than the Pb/Cd, implying that the value of Cd/Cu was more than unity. These suggest that smaller size humic aggregates were associated with Cu and Cd more than Pb, whereas larger humic aggregates were associated with Pb more than Cd and Cu. For humic aggregates in both Ca^{2+} solution and seawater at extended contact time (4,320 min), the values of Pb/Cd and Pb/Cu were closer to 1 as compared to the spiked humic acid, suggesting that in Ca^{2+} solution or seawater, all metal ions studied were more evenly distributed across size distribution of humic acid. In this study, elemental atomic ratios explained how metal ions were associated with humic aggregate in broad size range.

Conclusion

Owing to the fact that metal ions are associated with humic matter, mobility of metal ions in aquatic environment may be regulated by humic substances. Flow field-flow fractionation-ICP-MS offers a wide range of information, i.e., diameter; diffusion coefficient; and breadth of size distribution, which can be used to predict fate of metal ions interacted with humic matter. This study indicates that metal ions become less mobile in high salinity water, suggesting that metal mobility in fresh water should be faster than in estuarine or in seawater. The use of FlFFF-ICP-MS can be a comprehensive approach to help unravel the mystery of humic substances.

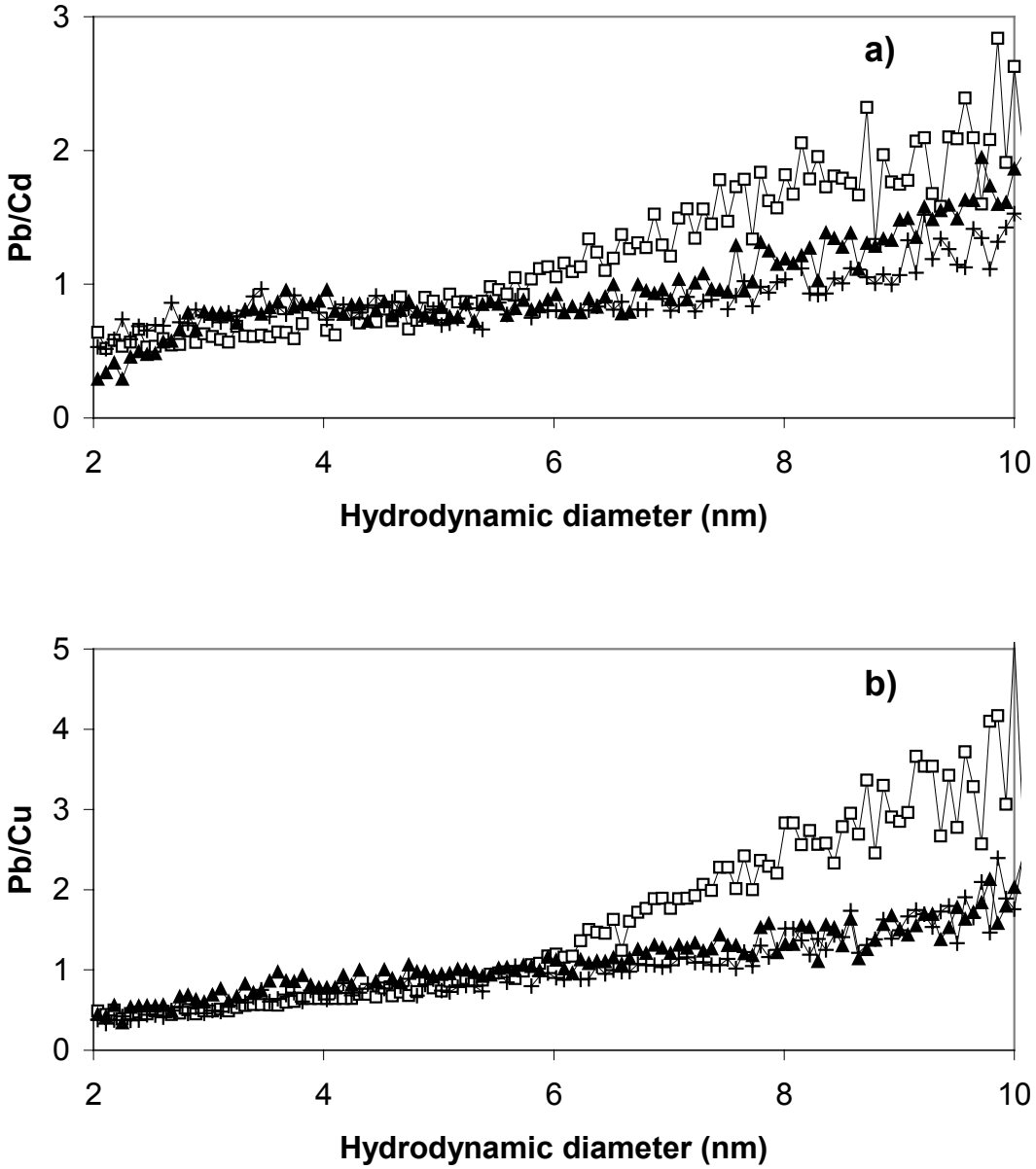

Figure 8 Elemental atomic ratio distributions: (a) Pb/Cd; and (b) Pb/Cu; in the spiked humic acid (—), spiked humic acid incubated in Ca^{2+} 1,600 mg/L for 4,320 min (■), and spiked humic acid incubated in seawater for 4,320 min (△).

References

1. Beckett, R. In *Surface and Colloid Chemistry in Natural Waters and Water Treatment*; Beckett, R., Ed.; Plenum Press: New York, 1990, pp 3-20.
2. Tipping, E. In *Cation Binding by Humic Substances*; Cambridge University Press: United Kingdom, 2002.
3. Piccolo, A. The supramolecular structure of humic substances. *Soil Sci*. 2001, *166*, 810-832.
4. Swift, R. S. Macromolecular properties of soil humic substances: fact, fiction, and opinion. *Soil Sci*. 1999, *164*, 790-802.
5. Schimpf, M. E.; Wahlund, K.-G. Asymmetrical flow field-flow fractionation as a method to study the behavior of humic acids. *J. Microcol. Sep*. 1997, *9*, 535-543.
6. Hine, P. T.; Bursill, D. B. Gel permeation chromatography of humic acid: problems associated with sephadex gel. *Water Res*. 1984, *18*, 1461-1468.
7. Yates, L. M.; von Wandruszka, R. Effects of pH and metals on the surface tension of aqueous humic materials. *Soil Sci. Soc. Am. J.* 1999, *63*, 1645-1649.
8. Ragle, C. S.; Engebretson, R. R.; von Wandruszka, R. The sequestration of hydrophobic micropollutants by dissolved humic acids. *Soil Sci*. 1997, *162*, 106-114.
9. Engebretson, R. R.; von Wandruszka, R. Kinetic aspects of cation-enhanced aggregation in aqueous humic acids. *Environ. Sci. Technol*. 1998, *32*, 488-493.
10. Amarasiriwardena, D.; Siripinyanond, A.; Barnes, R. M. In *Humic Substances: Versatile Components of Plants, Soil and Water*; Ghabbour, E. A., Davies, G., Eds.; The Royal Society of Chemistry: Cambridge, UK, 2000; pp 214-226.
11. Benincasa, M. A.; Cartoni, G.; Imperia, N. Effects of ionic strength and electrolyte composition on the aggregation of fractionated humic substances studied by flow field-flow fractionation. *J. Sep. Sci*. 2002, *25*, 405-415.
12. Wall, N. A.; Choppin, G. R. Humic acids coagulation: influence of divalent cations. *Appl. Geochem.*, 2003, *18*, 1573-1582.
13. Abbt-Braun, G.; Lankes, U.; Frimmel, F. H. Structural characterization of aquatic humic substances - the need for a multiple method approach. *Aquat. Sci.*, 2004, *66*, 151-170.

14. Perminova, I. V.; Frimmel, F. H.; Kovalevskii, D. V.; Abbt-Braun, G.; Kudryavtsev, A. V.; Hesse, S. Development of a predictive model for calculation of molecular weight of humic substances. *Water Res.* **1998**, *32*, 872-881.
15. Chin, Y. P.; Aiken, G. R.; O'Loughlin, E. Molecular weight, polydispersity, and spectroscopic properties of aquatic humic substances. *Environ. Sci. Technol.* **1994**, *28*, 1853-1858.
16. Peuravuori, J.; Pihlaja, K. Molecular size distribution and spectroscopic properties of aquatic humic substances. *Anal. Chim. Acta* **1997**, *337*, 133-149.
17. Wrobel, K.; Sadi, B. B. M.; Castillo, J. R.; Caruso, J. A. Effect of metal ions on the molecular weight distribution of humic substances derived from municipal compost: ultrafiltration and size exclusion chromatography with spectrophotometric and inductively coupled plasma-ms detection. *Anal. Chem.* **2003**, *75*, 761-767.
18. Hosse, M.; Wilkinson, K. J. Determination of electrophoretic mobilities and hydrodynamic radii of three humic substances as a function of ph and ionic strength. *Environ. Sci. Technol.*, **2001**, *35*, 4301-4306.
19. Sonke, J. E.; Salters, V. J. M. Determination of neodymium–fulvic acid binding constants by capillary electrophoresis inductively coupled plasma mass spectrometry (CE-ICP-MS). *J. Anal. At. Spectrom.*, **2004**, *19*, 235-240.
20. Beckett, R.; Zhang, J.; Giddings, J. C. Determination of molecular weight distributions of fulvic and humic acids using flow field-flow fractionation. *Environ. Sci. Technol.*, **1987**, *21*, 289-295.
21. Exner, A.; Theisen, M.; Panne, U.; Niessner, R. Combination of asymmetric flow field-flow fractionation (AF^4) and total-reflexion X-ray fluorescence analysis (TXRF) for determination of heavy metals associated with colloidal humic substances. *Fresenius' J. Anal. Chem.*, **2000**, *366*, 254-259.
22. Pelekani, C.; Newcombe, G.; Snoeyink, V. L.; Hepplewhite, C.; Assemi, S.; Beckett, R. Characterization of natural organic matter using high performance size exclusion chromatography. *Environ. Sci. Technol.* **1999**, *33*, 2807-2813.
23. Murphy, D. M.; Garbarino, J. R.; Taylor, H. E.; Hart, B. E.; Beckett, R. Determination of size and element composition distributions of complex colloids by sedimentation

field-flow fractionation-inductively coupled plasma mass spectrometry. *J. Chromatogr.* **1993**, *642*, 459-467.

24. Hassellöv, M.; Lyvén, B.; Beckett, R. Sedimentation field-flow fractionation coupled online to inductively coupled plasma mass spectrometry-new possibilities for studies of trace metal adsorption onto natural colloids. *Environ. Sci. Tech.*, **1999**, *33*, 4528-4531.
25. Ranville, J. F.; Chittleborough, D. J.; Shanks, F.; Morrison, R. J. S.; Harris, T.; Doss, F.; Beckett, R. Development of sedimentation field-flow fractionation-inductively coupled plasma mass-spectrometry for the characterization of environmental colloids. *Anal. Chim. Acta* **1999**, *381*, 315-329.
26. Schmitt, D.; Taylor, H. E.; Aiken, G. R.; Roth, D. A.; Frimmel, F. H. Influence of natural organic matter on the adsorption of metal ions onto clay minerals. *Environ. Sci. Technol.* **2002**, *36*, 2932-2938.
27. Lyvén, B.; Hassellöv, M.; Turner, D. R.; Haraldsson, C.; Andersson, K. Competition between iron- and carbon-based colloidal carriers for trace metals in a freshwater assessed using flow field-flow fractionation coupled to ICPMS. *Geochim. Cosmochim. Acta* **2003**, *67*, 3791-3802.
28. Amarasiriwardena, D.; Siripinyanond, A.; Barnes, R. M. Trace elemental distribution in soil and compost-derived humic acid molecular fractions and colloidal organic matter in municipal wastewater by flow field-flow fractionation-inductively coupled plasma mass spectrometry (flow FFF-ICP-MS). *J. Anal. At. Spectrom.* **2001**, *16*, 978-986.
29. Siripinyanond, A.; Barnes, R. M.; Amarasiriwardena, D. Flow field-flow fractionation-inductively coupled plasma mass spectrometry for sediment bound trace metal characterization. *J. Anal. At. Spectrom.*, **2002**, *17*, 1055-1064.
30. Beckett, R. Field-flow fractionation-ICP-MS: a powerful new analytical tool for characterizing macromolecules and particles. *Atom. Spectrosc.* **1991**, *12*, 228-232.
31. Taylor, H. E.; Garbarino, J. R.; Murphy, D. M.; Beckett, R. Inductively coupled plasma-mass spectrometry as an element-specific detector for field-flow fractionation particle separation. *Anal. Chem.* **1992**, *64*, 2036-2041.

32. Beckett, R.; Hart, B. T. In *Environmental Particles*; Buffle, F., van Leeuwen, H. P, Eds.; Lewis: Ann Arbor, MI, 1993; vol. 2, pp 165-205.
33. Schimpf, M. E.; Williams, P. S.; Giddings, J. C. Characterization of thermal diffusion in polymer solutions: dependence on polymer and solvent parameters. *J. Appl. Polym. Sci*. **1989**, *37*, 2059-2076.

Output ที่ได้จากโครงการ

Output ที่ได้จากโครงการ

สำหรับผลการดำเนินงานที่เห็นเป็นรูปธรรม สามารถแบ่งเป็น 3 หัวข้อต่าง ๆ ดังนี้

1. **การเสนอผลงานวิจัยในที่ประชุมนานาชาติ**

ได้นำเสนอผลงานวิจัยในที่ประชุมนานาชาติในหัวข้อที่เกี่ยวกับงานวิจัยในโครงการ 2 ครั้ง รวม 3 เรื่อง ดังนี้

1.1 The 2nd Asian International Conference on Ecotoxicology and Environmental Safety, Song-Khla, Thailand, September 28, 2004, Poster Number 36, “Field-flow fractionation-inductively coupled plasma mass spectrometry: an alternative approach to investigate metal-humic substances interaction”.

1.2 2005 Asia-Pacific Winter Conference on Plasma Spectrochemistry, Chiang Mai, Thailand, April 25 – 30, 2005, Poster Number WP11, “Elemental size characterization of air particulates using sedimentation field-flow fractionation-inductively coupled plasma optical emission spectrometry”.

1.3 2005 Asia-Pacific Winter Conference on Plasma Spectrochemistry, Chiang Mai, Thailand, April 25 – 30, 2005, Poster Number WP13, “Elemental size characterization of humic substances using flow field-flow fractionation-inductively coupled plasma mass spectrometry”.

2. **ผลงานวิจัยที่ตีพิมพ์ในวารสารวิชาการระดับนานาชาติ**

ได้ส่งผลงานวิจัยที่เกี่ยวข้องกับโครงการเพื่อตีพิมพ์ในวารสารนานาชาติ จำนวน 2 เรื่อง โดยที่ได้ตีพิมพ์แล้ว 1 เรื่อง ส่วนอีก 1 เรื่อง กำลังรอผลการพิจารณา

2.1 Siripinyanond, A.; Worapanyanond, S.; Shiowatana, J. Field-flow fractionation-inductively coupled plasma mass spectrometry: an alternative approach to investigate metal-humic substances interaction, *Environ. Sci. Technol.* **2005**, *39*,3295-3301. (Journal Impact Factor 3.59)

2.2 Kumtabtim, U.; Shiowatana, S.; Siripinyanond, A. Sedimentation field-flow fractionation-inductively coupled plasma optical emission spectrometry: size based elemental speciation of air particulates, *J. Anal. Atom. Spectrom.*, submitted. (Journal Impact Factor 3.93)

3. การพัฒนาศักยภาพในการทำงานวิจัย และผลงานวิจัยต่อเนื่อง

การได้รับทุนวิจัยเป็นจุดเริ่มในการทำงานวิจัยและพัฒนางานวิจัยให้มีความต่อเนื่อง ในระหว่างการทำงานวิจัยในโครงการ ได้องค์ความรู้ในการใช้เทคนิคการวิเคราะห์อนุภาค field-flow fractionation สามารถขยายผลเพื่อพัฒนาวิธีการวิเคราะห์นี้กับอนุภาคสารประเภทต่าง ๆ นอกเหนือจากอนุภาคสิ่งแวดล้อมที่ได้ทำการศึกษาในโครงการนี้ อนุภาคอื่น ๆ เช่น อนุภาคอาหาร ซึ่งคาดว่าจะเป็นงานต่อเนื่องในระยะหลังจากเสร็จสิ้นโครงการนี้

ภาคผนวก

Environ. Sci. Technol. **2005**, *39,* 3295−3301

Field-Flow Fractionation−Inductively Coupled Plasma Mass Spectrometry: An Alternative Approach to Investigate Metal−Humic Substances Interaction

ATITAYA SIRIPINYANOND,* SUMATTANA WORAPANYANOND, AND JUWADEE SHIOWATANA

Department of Chemistry, Faculty of Science, Mahidol University, Rama VI Road, Bangkok 10400, Thailand

Interaction between metal ions and humic matter was investigated using a hyphenated technique, field-flow fractionation−inductively coupled plasma mass spectrometry (FFF-ICP-MS). Aggregation of a metal-spiked commercial Aldrich humic acid in an aqueous solution of calcium ion or in seawater was examined over time intervals of 0−4320 min. The aggregation was demonstrated by shifts in peak maximum of humic matter from smaller size (2.9 nm) to larger size (5.1 or 5.8 nm in Ca^{2+} solution or in seawater, respectively) and also by the broadening of size distribution profiles. With FFF, size distribution of humic aggregate was characterized. Further, dominant particle size (2.9 nm), mean particle size (3.8 nm), and diffusion coefficient (1.51×10^{-6} cm^2/s) of humic acid solution were determined. With FFF-ICP-MS, associations of Cd, Cu, and Pb with humic aggregates were examined. The mean diameters of Cd-, Cu-, and Pb-bound humic aggregates in the metal-spiked humic acid were 4.1, 4.5, and 5.8 nm, respectively. These diameters were shifted to 6.0, 6.0, and 6.9 nm, respectively, in the humic acid incubated with calcium solution, whereas they were shifted to 6.5, 5.7, and 7.4 nm, respectively, in the humic acid incubated with seawater for three days. Humic aggregate of small size showed more affinity for Cu than Cd and Pb, whereas the large aggregate showed more affinity for Pb than Cd and Cu, respectively.

Introduction

Understanding the humic substances is one of the central issues of environmental studies, since they play vital roles in the regulation of nutrient and toxic elements in terrestrial and aquatic environments (*1*, *2*). Humic acids are thought to either be associations of relatively small molecules held together (*3*) or polymers exhibiting random coil conformation (*4*). Although the exact structure of humic acid is still controversial, it is reported to be very sensitive to pH and ionic strength changes (*5*−*7*). Only slight alterations in pH or ionic strength affect the structural conformation of humic macromolecules, and sometimes lead to humic aggregation (*5*, *8*−*11*) or flocculation (*12*). Detailed knowledge about humic aggregation phenomenon is still lacking. To investigate the aggregation, a reliable size separation technique is required. An overview of structural and size characterization method for humic substances was recently given (*13*). Numerous advanced analytical and separation techniques including vapor-pressure osmometry, high-pressure size-exclusion chromatography (HP-SEC) (*14*−*17*), capillary zone electrophoresis (CZE) (*18*, *19*), polyacrylamide gel electrophoresis (PAGE), analytical centrifugation, light scattering, mass spectrometry (MS), and flow field-flow fractionation (FlFFF) (*10*, *11*, *20*, *21*) have been reported for size characterization of humic materials. Nonetheless, discrepancies among methods were observed because of the measurement artifacts. Thus, puzzles of exact humic structure and size still remain to be solved. Among size-separation techniques, HP-SEC is the most commonly used approach. However, the potential interactions among humic acids with a stationary phase restrict the use of HP-SEC.

In this study, FlFFF was employed for the size characterization of humic acid. Although good agreement between the humic acid size data obtained from FlFFF and HP-SEC was demonstrated (*22*), the opportunity for humic molecules adsorption and degradation was minimized with the open channel characteristic (reduced surface area) of FlFFF in comparison with the packed HP-SEC column (*20*). With FlFFF, various facts on physicochemical properties of humic aggregate, i.e., diameter, size distribution, and diffusion coefficient, can be obtained. The purpose of this study is to investigate the aggregation of humic acid both in Ca^{2+} solution and in seawater. Further, an inductively coupled plasma (ICP) mass spectrometer was used as an element detector after humic size separation by FlFFF to investigate size distributions of Cd, Cu, and Pb binding humic acid aggregate. In addition, shifts in metal ions size distributions in the humic aggregates incubated in Ca^{2+} solution and seawater were observed to examine how these metal ions changed with humic aggregate size. A number of literatures on FFF-ICP-MS (*23*−*29*) have appeared since the technique was first proposed in 1991 (*30*) with the first experimental results reported in 1992 (*31*). Nonetheless, this study shows a novel application of FFF-ICP-MS and also suggests that the FFF-ICP-MS is an essential tool for characterization of metal−humic interaction.

Experimental Section

Chemicals and Molecular Weight Standards. A stock solution of 4000 mg/L Ca was prepared by dissolving 0.147 g of analytical reagent grade $CaCl_2 \cdot 2H_2O$ (Fisher Scientific, Co., Fair Lawn, NJ) in 10 mL of deionized water. Stock solutions of 100 mg/L Cd, Cu, and Pb were made by dissolving 0.0210, 0.0297, and 0.0207 g of $Cd(NO_3)_2$, $Cu(NO_3)_2$, and $Pb(NO_3)_2$ (Merck, Darmstadt, Germany) in 100 mL of deionized water. A 30 mM TRIS buffer was prepared by dissolving 3.6 g of tris(hydroxymethyl aminomethane) (Fisher Scientific, Ltd., Leicestershire, U.K.) in deionized water (1000 mL) and titrating to pH 7.5 with concentrated nitric acid.

Poly(styrene sulfonic acid sodium salt) molecular weight standards (1.4, 4.4, 15.2, and 43.3 kDa, Fluka Chemie GmbH., Switzerland) were used to calibrate the FlFFF channel. All standards were dissolved in 30 mM TRIS at pH 7.5.

Metal-Spiked Humic Acid. A commercial humic acid from an open pit mining area in Germany, purchased from Aldrich (Steinheim, Germany), was used in this study. The assays of the Aldrich humic acid are as follow: 39.0% C; 4.4% H; 3% S; 2% Na; 1.4% Fe; 0.5% Ca; 0.4% N; 0.4% Al; 0.05% Mg; 0.04%

* Corresponding author phone: +66-2-201-5129; fax: +66-2-354-7151; e-mail: scasp@mucc.mahidol.ac.th.

10.1021/es0483802 CCC: $30.25
Published on Web 03/18/2005

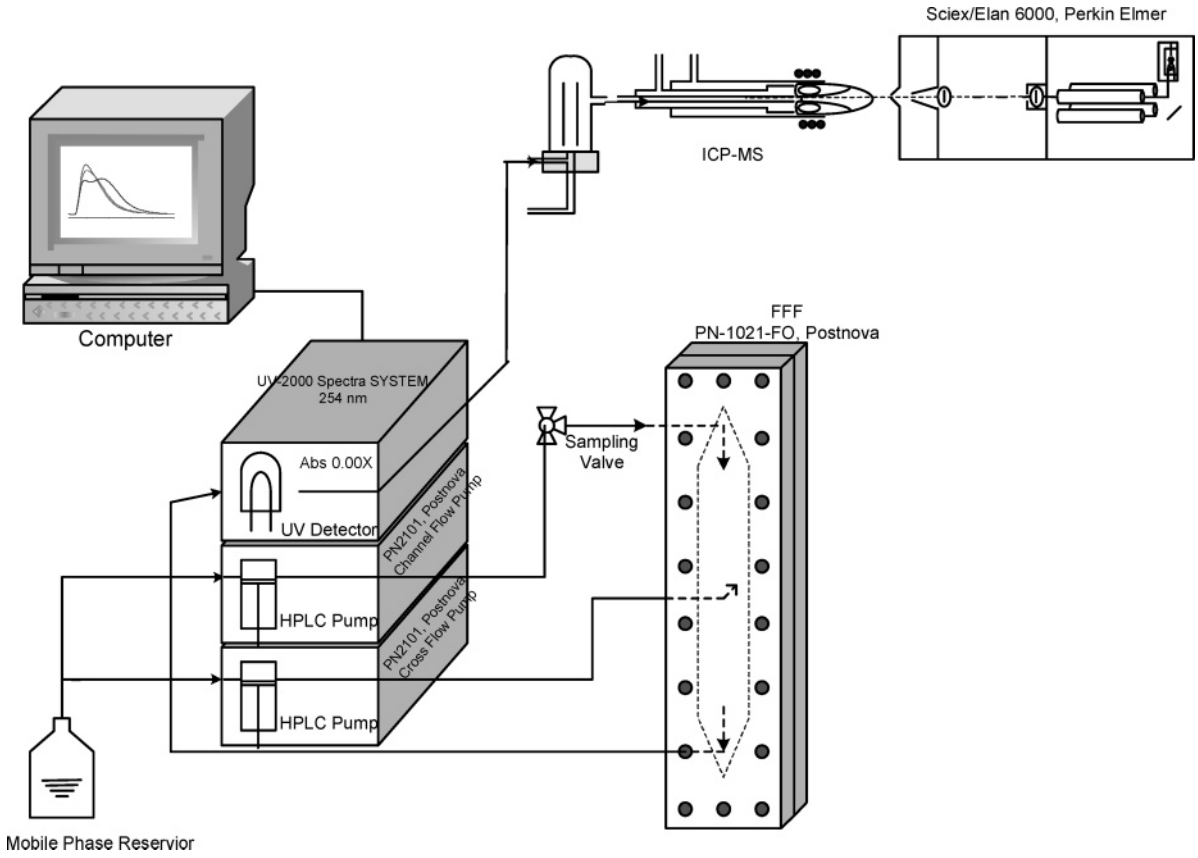

FIGURE 1. Schematic diagram illustrating FlFFF-ICP-MS arrangement. (After Siripinyanond et al. (*29*)).

K. A humic acid stock solution (6000 mg/L) was made by dissolving 0.060 g of the Aldrich humic acid in 10 mL of deionized water. A metal-spiked humic acid was prepared by mixing 5 mL of the dissolved Aldrich humic acid with the metal ion solutions and then making up to 10 mL with deionized water to contain 2, 6, and 2 mg/L of Cd, Cu, and Pb, respectively. This solution is hereafter referred to as "spiked humic acid". To study aggregation behavior of the spiked humic acid in the presence of Ca^{2+}, a 500-μL aliquot of humic acid solution was mixed with 400 μL of Ca^{2+} solution and made up with deionized water to obtain final humic acid concentration of 2000 mg/L and Ca^{2+} concentration of 1600 mg/L. To study aggregation behavior of the spiked humic acid in seawater, a 500-μL aliquot of spiked humic acid solution was mixed with seawater collected from the Jomtien Beach (Pattaya, Thailand) to obtain final humic acid concentration of 2000 mg/L.

Instrumentation. A FlFFF system (Model PN-1021-FO, Postnova Analytik, Germany) equipped with a 1-kDa molecular weight cut-off, regenerated cellulose acetate membrane (Postnova) was used. The FlFFF channel was 27.7 cm long, 2.0 cm wide, and 254 μm thick. The humic acid sample was injected directly into an injector valve (Rheodyne) with a fixed loop (20 μL) attached to the FlFFF channel front end. A 30 mM TRIS buffer (pH 7.5) was used as a carrier liquid throughout this study. A high-pressure liquid chromatography (HPLC) pump (Model PN 2101, Postnova Analytik, Germany) delivered the channel flow at 1 mL/min. Another HPLC pump of the same model was employed to regulate the cross-flow rate at 2 mL/min. A relaxation time of 2 min was allowed for sample particles situated at the top wall to move to the accumulation wall. The UV detector (UV-2000 Spectra SYSTEM) was set at 254 nm to monitor light attenuation of separated humic acid samples. An ICP mass spectrometer (Sciex/Elan 6000, PerkinElmer Instruments, Shelton, CT) was used as an element detector after the UV absorption detector as illustrated in Figure 1. Because of the similarity of the FlFFF channel flow and ICP-MS sampling flow rates typically used for analysis, the ICP mass spectrometer cross-flow nebulizer was connected directly to the UV detector outlet with a 35-cm length of poly(tetrafluoroethylene) tubing (PTFE, 0.58 mm inside diameter). The FlFFF-ICP-MS operating conditions are summarized in Table 1.

Observation of Humic Acid Aggregation. The aggregation at room temperature was observed immediately after mixing calcium ion solution, or seawater, with humic solutions. Recording of data was performed at appropriate intervals of 1, 60, 180, 300, and 4320 min.

Data Transformation. Raw fractograms were translated into size distribution profiles using an Excel (Microsoft Excel 2002, Redmond, WA) spreadsheet. Peak area normalization and cumulative area determination were performed using PeakFit (SPSS, Chicago, IL).

Results and Discussion

Particle Size Characteristics: Evidence on Humic Aggregation. To obtain the information about the hydrodynamic size of humic acid, retention times (t_r) of a raw fractogram were translated into hydrodynamic diameters (d_h). Consequently, the raw fractograms were converted into the hydrodynamic size distributions using the method described by Beckett et al. (*32*) and Schimpf et al. (*33*). Once the size distribution profile was plotted, particle size at peak maximum (d_p), breadth of size distributions ($\Delta d_{0.5}$), and mean particle size (d_{mean}) were measured.

Particle size at peak maximum (d_p) was used to identify the dominant particle size of the investigated humic acid. To quantify the breadth of size distributions, particle size ranges at half-maximum height ($\Delta d_{0.5}$) were calculated from the distribution profiles. The measured d_p and $\Delta d_{0.5}$ values for

TABLE 1. FlFFF-ICP-MS Operating Conditions

Flow FFF Model PN-1021-FO	
FFF channel dimensions (cm)	27.7 long × 2.0 wide × 0.02 cm thick
carrier liquid	30 mM TRIS (buffered at pH 7.5)
channel flow rate (mL/min)	1.0
cross-flow rate (mL/min)	2.0
equilibration time (min)	2.0
membrane	1 kDa MWCO poly(regenerated cellulose acetate)
ICP-MS Elan 6000	
R_f generator frequency (MHz)	40
R_f forward power (W)	1000
torch	Fassel type
torch injector	ceramic alumina
spray chamber	Ryton Scott double pass
nebulizer	gem-tip cross-flow
nebulizer gas flow rate (L/min)	0.95
intermediate gas flow rate (L/min)	1.2
outer gas flow rate (L/min)	15
resolution	1 ± 0.1 at 10% peak maximum
scanning mode	peak hop transient signal
measurement per peak	1
dwell time (ms)	200
isotopes monitored (*m*/*z*)	^{63}Cu, ^{65}Cu, ^{111}Cd, ^{114}Cd, ^{206}Pb, ^{208}Pb

TABLE 2. Particle Size Information of Humic Aggregate

contact time (min)	d_p	d_{mean}	$\Delta d_{0.5}$
Humic Aggregate in Ca^{2+} solution			
0	2.9	3.8	3.1
60	3.1	4.2	3.7
180	3.3	4.5	4.2
300	3.6	4.6	4.5
4320	2.8 and 5.1	5.2	5.8
Humic Aggregate in Seawater			
0	2.9	3.8	3.1
60	2.9	4.2	3.9
180	2.9 and 5.2	4.8	4.8
300	2.8 and 5.4	4.9	5.1
4320	2.8 and 5.8	5.1	5.3

humic aggregates in Ca^{2+} solution and in seawater at various contact times are summarized in Table 2. To obtain the mean particle size (d_{mean}) of humic aggregates, the diameter distribution profiles (Figure 2) were converted into cumulative area plots as shown in Figure 3. The d_{mean} is defined as the particle size at which 50% of the total accumulative area is detected. The d_{mean} values were determined from the cumulative plots, as summarized in Table 2. To illustrate the measurement precision, size characterization of humic acid without addition of Ca^{2+} or seawater was performed nine times, and the results are as follows: $d_p = 2.90 \pm 0.05$; $d_{mean} = 3.80 \pm 0.03$; $\Delta d_{0.5} = 3.10 \pm 0.08$.

In this study, particle size information obtained from FlFFF is used to provide evidence on humic aggregation. The aggregation phenomenon of humic acid (2000 mg/L) in the presence of Ca^{2+} (1600 mg/L) was temporally investigated as demonstrated by shifts in size distributions with increasing contact time (Figure 2a). With increasing contact time between humic acid and Ca^{2+}, the size distributions slightly broadened and yielded a bimodal size distribution characteristic at extended contact time (4320 min). The peak maxima appeared at longer retention times or at larger diameter sizes (Figure 2a and Table 2), providing a clear evidence of humic aggregation. Particle size at peak maximum (d_p), mean particle size (d_{mean}), and breadth of size distributions ($\Delta d_{0.5}$) increased with increasing contact time, suggesting that the aggregation process gradually took place. In seawater, however, d_{mean} and $\Delta d_{0.5}$ increased, whereas the d_p remained constant with increasing contact time. This finding suggests that, in order to observe humic acid aggregation, information

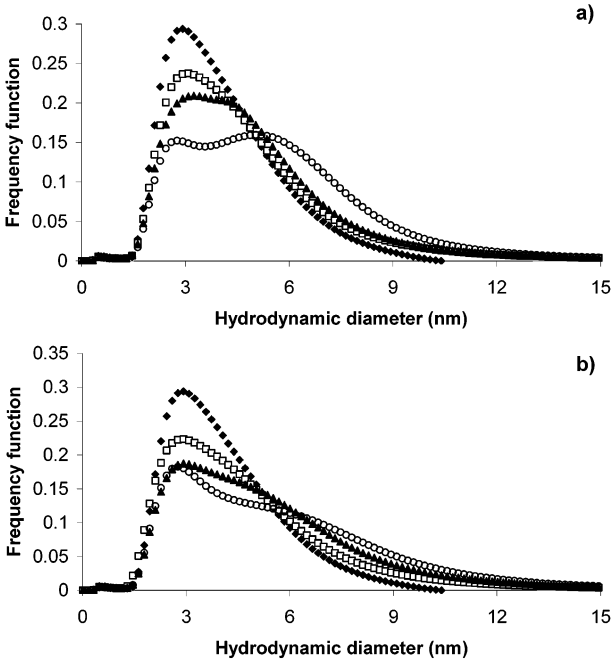

FIGURE 2. Hydrodynamic diameter distributions of humic acid (2000 mg/L) in (a) Ca^{2+} 1600 mg/L and (b) seawater at 0 (◆), 60 (□), 180 (▲), and 4320 min (○) contact times. (Because of the similarity between the hydrodynamic diameter distributions of humic acids at 180- and 300-min contact times, the hydrodynamic diameter distribution of humic acid at the 300-min contact time is not shown.)

on particle size at peak maximum (d_p) only is not adequate. The d_{mean} and $\Delta d_{0.5}$ also should be considered. In seawater medium, the bimodal characteristic was initially observed at contact time of 180 min (Figure 2b). At 180 min contact time, the dominant hydrodynamic sizes were observed at 2.9 and 5.2 nm. The former remained constant and the latter increased with increasing contact time. These could suggest that aggregation only occurred with humic matter of larger sizes.

Diffusion Coefficients of Humic Aggregate. FlFFF also provides information on diffusion properties of humic acid (*10*, *20*). Diffusion coefficient of humic aggregate is an inverse function of hydrodynamic diameter as follows: $D = kT/3\pi\eta d_h$; where k is the Boltzmann's constant (1.38×10^{-16} g

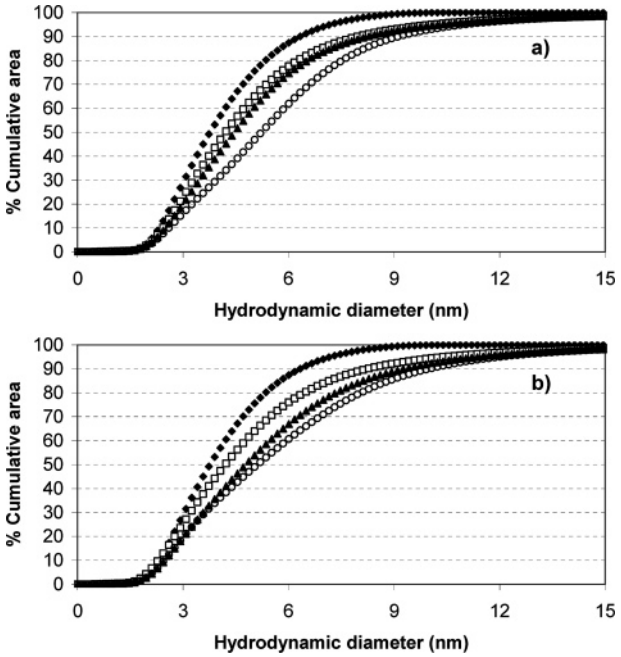

FIGURE 3. Cumulative area plots for humic acid (2000 mg/L) in (a) Ca^{2+} 1600 mg/L and (b) seawater at 0 (◆), 60 (□), 180 (▲), and 4320 min (○) contact times. (Because of the similarity between the cumulative area plots for humic acids at 180- and 300-min contact times, the cumulative area plot for humic acid at the 300-min contact time is not shown.)

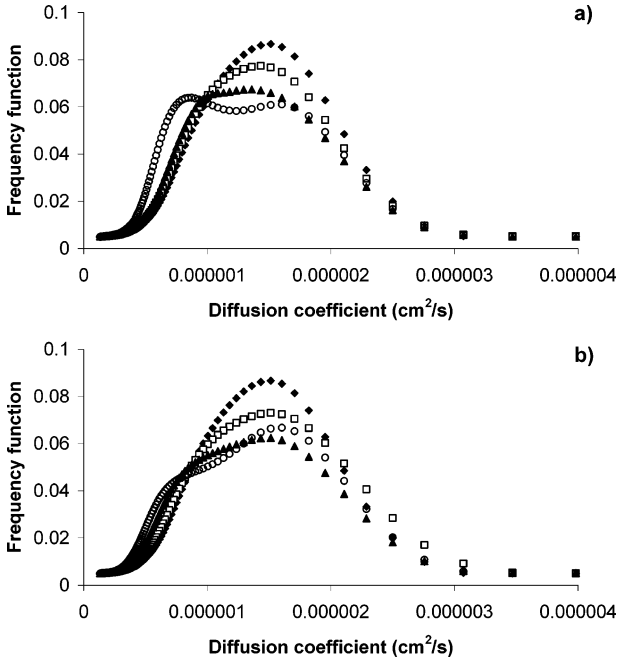

FIGURE 4. Diffusion coefficient distributions of humic acid (2000 mg/L) in (a) Ca^{2+} 1600 mg/L and (b) seawater at 0 (◆), 60 (□), 180 (▲), and 4320 min (○) contact times. (Because of the similarity between the diffusion coefficient distributions of humic acids at 180- and 300-min contact times, diffusion coefficient distribution of humic acid at the 300-min contact time is not shown.)

TABLE 3. Diffusion Coefficients of Humic Aggregate

contact time (min)	D_p	D_{mean}	D_{mean}/D_p
	Ca^{2+} Solution		
0	1.51×10^{-6}	1.51×10^{-6}	1
60	1.43×10^{-6}	1.47×10^{-6}	1.03
180	1.34×10^{-6}	1.41×10^{-6}	1.05
300	1.22×10^{-6}	1.41×10^{-6}	1.16
4320	0.87×10^{-6}	1.40×10^{-6}	1.61
	Seawater		
0	1.51×10^{-6}	1.51×10^{-6}	1
60	1.51×10^{-6}	1.56×10^{-6}	1.03
180	1.49×10^{-6}	1.45×10^{-6}	0.97
300	1.56×10^{-6}	1.47×10^{-6}	0.94
4320	1.58×10^{-6}	1.51×10^{-6}	0.96

$cm^2/s^2\ K^1$), T is absolute temperature (K), and η is the carrier liquid viscosity (g/cm s). In this study, diffusion coefficient at peak (D_p) and mean diffusion coefficient (D_{mean}) of humic aggregates were computed as summarized in Table 3. Distribution of diffusion coefficient also was plotted as illustrated in Figure 4. The experimentally obtained values of D_p are in the same order of magnitude as what reported by other investigators (*20*). Particles or macromolecules of larger size exhibit less diffusion coefficients than the smaller counterparts. In Ca^{2+} solution, D_{mean} decreased with increasing contact time, implying that the humic aggregate became less mobile in the presence of calcium ion. Furthermore, the ratio between D_{mean} and D_p is proposed here to describe the degree of normal distribution. A ratio of 1 indicates a symmetrical normal distribution profile, whereas a ratio deviating from 1 suggests the presence of distribution asymmetry. The D_{mean}/D_p of humic aggregate at contact times up to 3 h were close to unity, indicating normal distribution profiles of the diffusion coefficient values. Nonetheless, the ratios deviated from unity with increasing contact time, suggesting that the diffusion coefficient values deviated from normal distribution as the larger aggregates were gradually formed.

Size Distributions of Metal-Ion-Bound Humic Acid. Association of metal ions with humic aggregates was observed using FlFFF-ICP-MS. The ion fractograms of Cd, Cu, and Pb were obtained by ICP-MS detection after size separation of humic aggregates by FlFFF. The ion fractograms were then translated into hydrodynamic size distributions. The normalized size distributions of Cd-, Cu-, and Pb-bound humic aggregates in Ca^{2+} solution or seawater are shown in Figures 5 and 6, respectively. Once the elemental profile showing size distribution of metal-ion-bound humic aggregates was plotted, particle size at peak maximum (d_p), breadth of size distributions ($\Delta d_{0.5}$), and mean particle size (d_{mean}) of each metal ion were measured, as summarized in Table 4. In both Ca^{2+} solution and seawater, d_p, d_{mean}, and $\Delta d_{0.5}$ of Pb-bound humic aggregates were larger than those of Cd and those of Cu. The findings, in which the d_p and d_{mean} of Pb-bound humic aggregates were largest, suggest that large humic aggregate has more affinity for Pb than Cd and Cu, whereas small humic aggregate has more affinity for Cu than Cd and Pb. The $\Delta d_{0.5}$ value of Pb-bound humic aggregates was largest, implying that the hydrodynamic sizes of Pb were more dispersed in comparison with those of Cd and Cu. For a closer look of the $\Delta d_{0.5}$ values, Cd- and Cu-bound humic aggregates exhibited the same degree of size distribution breadth for the spiked humic acid (without addition of Ca^{2+} or seawater) and the spiked humic acid in both Ca^{2+} solution and seawater at extended contact time (4320 min). However, the size distributions of Cu-bound humic aggregates were narrower than those of Cd at contact times of less than 5 h. These suggest that the hydrodynamic sizes of Cu-bound humic aggregates were less dispersed than those of Cd. At extended contact time, broader size distributions of all metal-ion-bound humic aggregates were observed in seawater as compared to in Ca^{2+} solution. This is especially true for Pb-bound humic aggregates, whose size distribution breadth is equal to 6.6 or 8.7 in Ca^{2+} solution or in seawater, respectively. Therefore, a conclusion is made that all metal-ions-bound humic

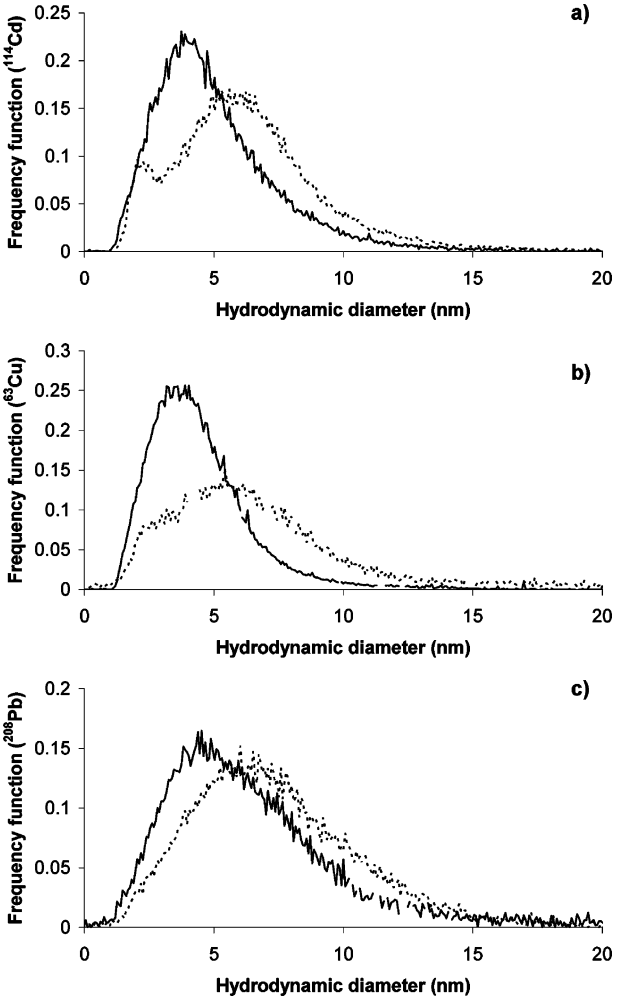

FIGURE 5. Hydrodynamic diameter distributions of (a) ^{114}Cd-, (b) ^{63}Cu-, and (c) ^{208}Pb-bound humic aggregates in the spiked humic acid (solid line) and spiked humic acid incubated in Ca^{2+} 1600 mg/L for 4320 min (dotted line).

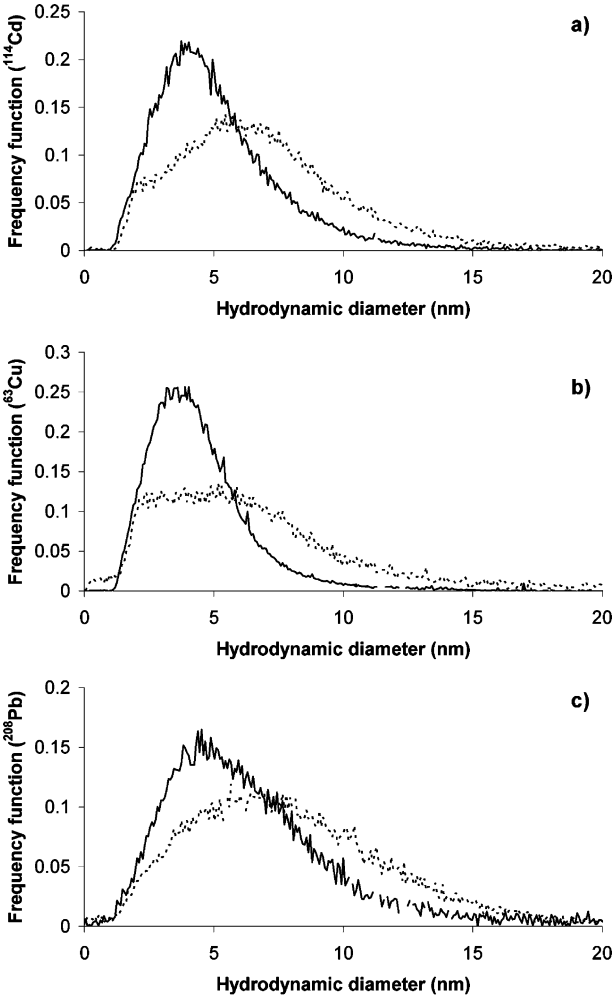

FIGURE 6. Hydrodynamic diameter distributions of (a) ^{114}Cd-, (b) ^{63}Cu-, and (c) ^{208}Pb-bound humic aggregates in the spiked humic acid (solid line) and spiked humic acid incubated in seawater for 4320 min (dotted line).

aggregates were dimensionally more dispersed in seawater than in Ca^{2+} solution.

To examine how metal ions are distributed in each humic size fraction, size distribution profiles of humic acid, and Cd-, Cu-, and Pb-bound humic aggregates were plotted together, as illustrated in Figure 7. In the spiked humic acid, Cd- and Cu-bound humic acid size distributions followed humic size distribution quite well with a slight shift in peak maxima (d_p of humic, Cd, and Cu were 2.9, 4.0, and 3.7 nm, respectively), whereas Pb-bound humic aggregates show broader size range with a significant shift in peak maximum (d_p of Pb-bound humic acid was 4.6 nm, see Figure 7a). These are the evidences that metal ions have the preference to associate with larger humic aggregates than the smaller counterparts.

Furthermore, the mean diameter ratio between metal-ion-bound humic aggregate and humic aggregate was

TABLE 4. Particle Size Information of Metal Ions in Humic Aggregate[a]

contact time (min)	$d_{p[Cd]}$	$d_{p[Cu]}$	$d_{p[Pb]}$	$d_{mean[Cd]}$	$d_{mean[Cu]}$	$d_{mean[Pb]}$	$\Delta d_{0.5[Cd]}$	$\Delta d_{0.5[Cu]}$	$\Delta d_{0.5[Pb]}$
Humic Aggregate in Ca^{2+} Solution									
0	4.0	3.7	4.6	4.5	4.1	5.8	3.8	3.9	5.4
60	4.5	4.0	5.4	5.1	4.2	6.3	3.9	3.5	6.2
180	4.7	4.3	5.7	5.5	4.7	6.7	4.5	3.6	6.5
300	5.0	4.5	5.9	5.5	4.8	6.8	4.7	3.8	6.9
4320	5.6	5.5	6.3	6.0	6.0	6.9	6.3	6.3	6.6
Humic Aggregate in Seawater									
0	4.0	3.7	4.6	4.5	4.1	5.8	3.8	3.9	5.4
60	4.7	3.9	5.4	5.2	4.4	6.3	4.9	4.0	6.4
180	5.2	4.5	6.6	6.0	5.0	7.2	5.4	4.3	7.5
300	5.5	4.7	6.7	6.1	5.2	7.4	5.6	4.8	7.7
4320	6.0	4.7	6.6	6.5	5.7	7.4	6.9	6.9	8.7

[a] $d_{p[Cd]}$, $d_{mean[Cd]}$, or $\Delta d_{0.5[Cd]}$ represents d_p, d_{mean}, or $\Delta d_{0.5}$, respectively, of Cd in humic aggregate. $d_{p[Cu]}$, $d_{mean[Cu]}$, or $\Delta d_{0.5[Cu]}$ represents d_p, d_{mean}, or $\Delta d_{0.5}$, respectively, of Cu in humic aggregate. $d_{p[Pb]}$, $d_{mean[Pb]}$, or $\Delta d_{0.5[Pb]}$ represents d_p, d_{mean}, or $\Delta d_{0.5}$, respectively, of Pb in humic aggregate.

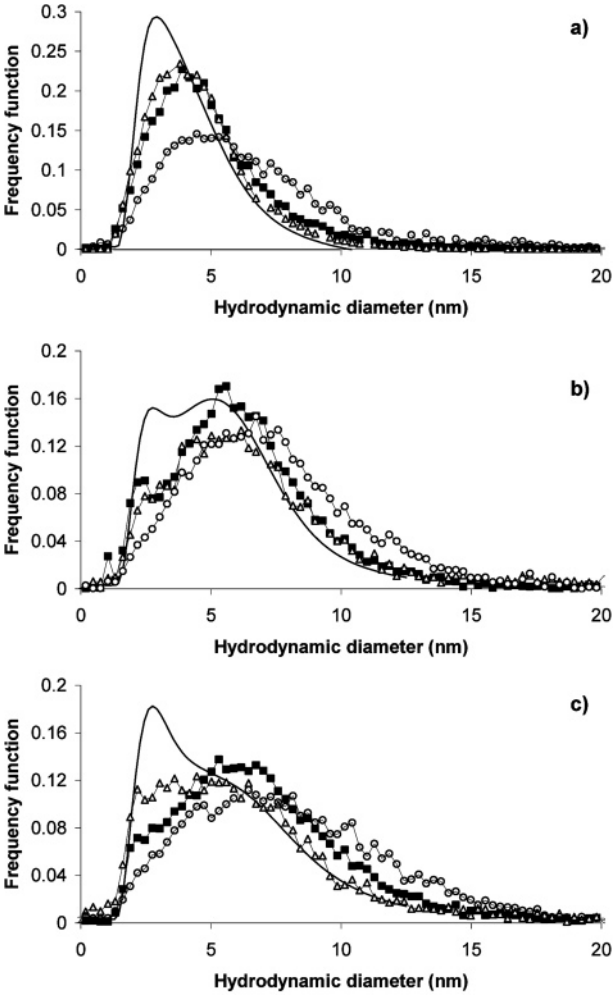

FIGURE 7. Hydrodynamic diameter distributions of humic acid (solid line) and the associated metal ions, i.e., ^{114}Cd (△), ^{63}Cu (■), and ^{208}Pb (○): (a) the spiked humic acid; (b) spiked humic acid incubated in Ca^{2+} 1600 mg/L for 4320 min; and (c) spiked humic acid incubated in seawater for 4320 min.

TABLE 5. Mean Diameter Ratios between Metal Ion and Humic Aggregate

contact time (min)	$d_{mean[Cd/humic]}$	$d_{mean[Cu/humic]}$	$d_{mean[Pb/humic]}$
	Humic Aggregate in Ca^{2+} Solution		
0	1.18	1.08	1.53
60	1.21	1.00	1.50
180	1.22	1.04	1.49
300	1.20	1.04	1.48
4320	1.15	1.15	1.33
	Humic Aggregate in Seawater		
0	1.18	1.08	1.53
60	1.24	1.05	1.50
180	1.25	1.04	1.50
300	1.24	1.06	1.51
4320	1.27	1.12	1.45

[a] $d_{mean[Cd/humic]}$ represents the mean diameter ratio between Cd and humic aggregate. $d_{mean[Cu/humic]}$ represents the mean diameter ratio between Cu and humic aggregate. $d_{mean[Pb/humic]}$ represents the mean diameter ratio between Pb and humic aggregate.

calculated, as summarized in Table 5. This value can be used as an index to predict how metal is distributed across humic size range. A value of 1 indicates that the metal ions are distributed evenly across humic size range, and a value higher than 1 suggests that the metal ions are associated more with

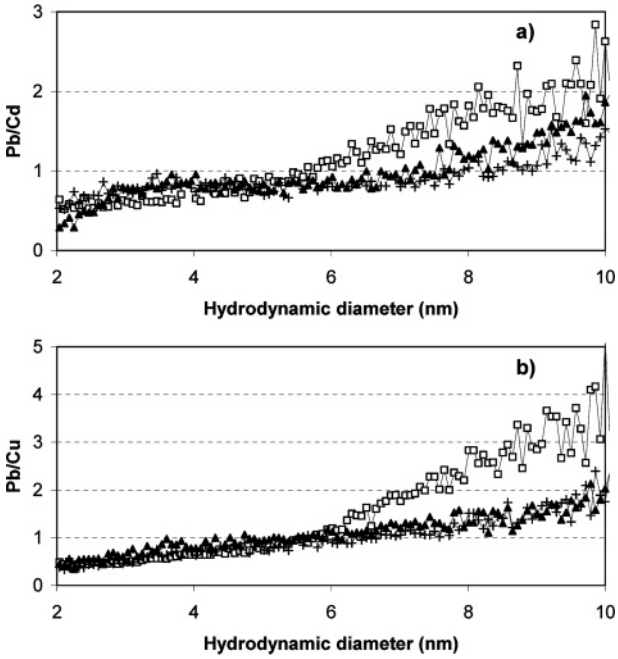

FIGURE 8. Elemental atomic ratio distributions: (a) Pb/Cd; and (b) Pb/Cu; in the spiked humic acid (solid line), spiked humic acid incubated in Ca^{2+} 1600 mg/L for 4320 min (△), and spiked humic acid incubated in seawater for 4320 min (■).

larger size than the smaller size aggregate. Conversely, the value less than 1 implies that the metal ions are associated more with smaller size than the larger size aggregate. The mean diameter ratio of Cu was close to unity, suggesting that Cu-bound humic acid size distribution was well correlated with size distribution of humic acid. Size distributions of Pb-bound humic aggregates, however, were less correlated with humic size distribution, as compared to those of Cu and Cd.

Elemental Ratios Across Size Distribution. Murphy et al. (*23*) and Hassellöv et al. (*24*) suggested that the elemental atomic ratio distributions could be used to follow changes in chemical composition of mixtures as a function of particle size. In Figure 8, the elemental atomic ratios are plotted against hydrodynamic diameters. The Pb/Cd and Pb/Cu for the spiked humic acid (without addition of Ca^{2+} or seawater) were less than 1 in the size range between 2 and 5 nm and were larger than 1 in the hydrodynamic diameters larger than 6 nm. The Pb/Cu was higher than the Pb/Cd, implying that the value of Cd/Cu was more than unity. These suggest that smaller size humic aggregates were associated with Cu and Cd more than Pb, whereas larger humic aggregates were associated with Pb more than Cd and Cu. For humic aggregates in both Ca^{2+} solution and seawater at extended contact times (4320 min), the values of Pb/Cd and Pb/Cu were closer to 1 as compared to the spiked humic acid, suggesting that, in Ca^{2+} solution or seawater, all metal ions studied were more evenly distributed across size distribution of humic acid. In this study, elemental atomic ratios explained how metal ions were associated with humic aggregate in broad size range.

FlFFF-ICP-MS and the Mystery of Humic Substances. Because metal ions are associated with humic matter, mobility of metal ions in aquatic environment may be regulated by humic substances. FlFFF-ICP-MS offers a wide range of information, i.e., diameter, diffusion coefficient, and breadth of size distribution, which can be used to predict fate of metal ions interacted with humic matter. This study indicates that metal ions become less mobile in high salinity water, suggesting that metal mobility in freshwater should

be faster than in estuarine or in seawater. The use of FlFFF-ICP-MS can be a comprehensive approach to help unravel the mystery of humic substances.

Acknowledgments

The Postgraduate Education and Research Program in Chemistry is gratefully acknowledged for the studentship support for S.W., the partial research support for A.S., and the purchase of the FFF equipment. Thanks are also due to the Thailand Research Fund for the research support for A.S. and to Miss Weerawan Waiyawat for her help in ICP-MS system optimization. This paper was presented in part at the 2nd Asian International Conference on Ecotoxicology and Environmental Safety, Song-Khla, Thailand, September 28, 2004, Poster Number 36.

Literature Cited

(1) Beckett, R. In *Surface and Colloid Chemistry in Natural Waters and Water Treatment*; Beckett, R., Ed.; Plenum Press: New York, 1990; pp 3−20.
(2) Tipping, E. In *Cation Binding by Humic Substances*; Cambridge University Press: United Kingdom, 2002.
(3) Piccolo, A. The supramolecular structure of humic substances. *Soil Sci.* **2001**, *166*, 810−832.
(4) Swift, R. S. Macromolecular properties of soil humic substances: fact, fiction, and opinion. *Soil Sci.* **1999**, *164*, 790−802.
(5) Schimpf, M. E.; Wahlund, K.-G. Asymmetrical flow field-flow fractionation as a method to study the behavior of humic acids. *J. Microcolumn Sep.* **1997**, *9*, 535−543.
(6) Hine, P. T.; Bursill, D. B. Gel permeation chromatography of humic acid: problems associated with sephadex gel. *Water Res.* **1984**, *18*, 1461−1468.
(7) Yates, L. M.; von Wandruszka, R. Effects of pH and metals on the surface tension of aqueous humic materials. *Soil Sci. Soc. Am. J.* **1999**, *63*, 1645−1649.
(8) Ragle, C. S.; Engebretson, R. R.; von Wandruszka, R. The sequestration of hydrophobic micropollutants by dissolved humic acids. *Soil Sci.* **1997**, *162*, 106−114.
(9) Engebretson, R. R.; von Wandruszka, R. Kinetic aspects of cation-enhanced aggregation in aqueous humic acids. *Environ. Sci. Technol.* **1998**, *32*, 488−493.
(10) Amarasiriwardena, D.; Siripinyanond, A.; Barnes, R. M. In *Humic Substances: Versatile Components of Plants, Soil and Water*; Ghabbour, E. A., Davies, G., Eds.; The Royal Society of Chemistry: Cambridge, UK, 2000; pp 214−226.
(11) Benincasa, M. A.; Cartoni, G.; Imperia, N. Effects of ionic strength and electrolyte composition on the aggregation of fractionated humic substances studied by flow field-flow fractionation. *J. Sep. Sci.* **2002**, *25*, 405−415.
(12) Wall, N. A.; Choppin, G. R. Humic acids coagulation: influence of divalent cations. *Appl. Geochem.* **2003**, *18*, 1573−1582.
(13) Abbt-Braun, G.; Lankes, U.; Frimmel, F. H. Structural characterization of aquatic humic substances - the need for a multiple method approach. *Aquat. Sci.* **2004**, *66*, 151−170.
(14) Perminova, I. V.; Frimmel, F. H.; Kovalevskii, D. V.; Abbt-Braun, G.; Kudryavtsev, A. V.; Hesse, S. Development of a predictive model for calculation of molecular weight of humic substances. *Water Res.* **1998**, *32*, 872−881.
(15) Chin, Y. P.; Aiken, G. R.; O'Loughlin, E. Molecular weight, polydispersity, and spectroscopic properties of aquatic humic substances. *Environ. Sci. Technol.* **1994**, *28*, 1853−1858.
(16) Peuravuori, J.; Pihlaja, K. Molecular size distribution and spectroscopic properties of aquatic humic substances. *Anal. Chim. Acta* **1997**, *337*, 133−149.
(17) Wrobel, K.; Sadi, B. B. M.; Castillo, J. R.; Caruso, J. A. Effect of metal ions on the molecular weight distribution of humic substances derived from municipal compost: ultrafiltration and size exclusion chromatography with spectrophotometric and inductively coupled plasma-ms detection. *Anal. Chem.* **2003**, *75*, 761−767.
(18) Hosse, M.; Wilkinson, K. J. Determination of electrophoretic mobilities and hydrodynamic radii of three humic substances as a function of pH and ionic strength. *Environ. Sci. Technol.* **2001**, *35*, 4301−4306.
(19) Sonke, J. E.; Salters, V. J. M. Determination of neodymium-fulvic acid binding constants by capillary electrophoresis inductively coupled plasma mass spectrometry (CE-ICP-MS). *J. Anal. At. Spectrom.* **2004**, *19*, 235−240.
(20) Beckett, R.; Zhang, J.; Giddings, J. C. Determination of molecular weight distributions of fulvic and humic acids using flow field-flow fractionation. *Environ. Sci. Technol.* **1987**, *21*, 289−295.
(21) Exner, A.; Theisen, M.; Panne, U.; Niessner, R. Combination of asymmetric flow field-flow fractionation (AF^4) and total-reflection X-ray fluorescence analysis (TXRF) for determination of heavy metals associated with colloidal humic substances. *Fresenius' J. Anal. Chem.* **2000**, *366*, 254−259.
(22) Pelekani, C.; Newcombe, G.; Snoeyink, V. L.; Hepplewhite, C.; Assemi, S.; Beckett, R. Characterization of natural organic matter using high performance size exclusion chromatography. *Environ. Sci. Technol.* **1999**, *33*, 2807−2813.
(23) Murphy, D. M.; Garbarino, J. R.; Taylor, H. E.; Hart, B. E.; Beckett, R. Determination of size and element composition distributions of complex colloids by sedimentation field-flow fractionation-inductively coupled plasma mass spectrometry. *J. Chromatogr.* **1993**, *642*, 459−467.
(24) Hassellöv, M.; Lyvén, B.; Beckett, R. Sedimentation field-flow fractionation coupled online to inductively coupled plasma mass spectrometry-new possibilities for studies of trace metal adsorption onto natural colloids. *Environ. Sci. Technol.* **1999**, *33*, 4528−4531.
(25) Ranville, J. F.; Chittleborough, D. J.; Shanks, F.; Morrison, R. J. S.; Harris, T.; Doss, F.; Beckett, R. Development of sedimentation field-flow fractionation-inductively coupled plasma mass-spectrometry for the characterization of environmental colloids. *Anal. Chim. Acta* **1999**, *381*, 315−329.
(26) Schmitt, D.; Taylor, H. E.; Aiken, G. R.; Roth, D. A.; Frimmel, F. H. Influence of natural organic matter on the adsorption of metal ions onto clay minerals. *Environ. Sci. Technol.* **2002**, *36*, 2932−2938.
(27) Lyvén, B.; Hassellöv, M.; Turner, D. R.; Haraldsson, C.; Andersson, K. Competition between iron- and carbon-based colloidal carriers for trace metals in a freshwater assessed using flow field-flow fractionation coupled to ICPMS. *Geochim. Cosmochim. Acta* **2003**, *67*, 3791−3802.
(28) Amarasiriwardena, D.; Siripinyanond, A.; Barnes, R. M. Trace elemental distribution in soil and compost-derived humic acid molecular fractions and colloidal organic matter in municipal wastewater by flow field-flow fractionation-inductively coupled plasma mass spectrometry (flow FFF−ICP-MS). *J. Anal. At. Spectrom.* **2001**, *16*, 978−986.
(29) Siripinyanond, A.; Barnes, R. M.; Amarasiriwardena, D. Flow field-flow fractionation-inductively coupled plasma mass spectrometry for sediment bound trace metal characterization. *J. Anal. At. Spectrom.* **2002**, *17*, 1055−1064.
(30) Beckett, R. Field-flow fractionation-ICP-MS: a powerful new analytical tool for characterizing macromolecules and particles. *Atom. Spectrosc.* **1991**, *12*, 228−232.
(31) Taylor, H. E.; Garbarino, J. R.; Murphy, D. M.; Beckett, R. Inductively coupled plasma-mass spectrometry as an element-specific detector for field-flow fractionation particle separation. *Anal. Chem.* **1992**, *64*, 2036−2041.
(32) Beckett, R.; Hart, B. T. In *Environmental Particles*; Buffle, F., van Leeuwen, H. P., Eds.; Lewis: Ann Arbor, MI, 1993; Vol. 2, pp 165−205.
(33) Schimpf, M. E.; Williams, P. S.; Giddings, J. C. Characterization of thermal diffusion in polymer solutions: dependence on polymer and solvent parameters. *J. Appl. Polym. Sci.* **1989**, *37*, 2059−2076.

Received for review October 18, 2004. Revised manuscript received December 31, 2004. Accepted February 11, 2005.

ES0483802